POLITECNICO DI TORINO

Corso di Laurea Magistrale in Ingegneria per l'Ambiente e il Territorio

Tesi di Laurea Magistrale

Mobility of aluminium-OM flocs in porous media and their ability to reduce the hydraulic conductivity

Analisi della mobilità di aggregati di alluminio e materia organica nel mezzo poroso e della loro capacità di ridurre la conducibilità idraulica.

Relatori: Prof. Tiziana Tosco, Rajandrea Sethi, Carlo Bianco e Susanne Laumann

Candidato: Valentina Sanna

Progetto di tesi sviluppato all'estero presso TU Delft

Anno Accademico 2019-2020

Abstract

The Netherlands must tackle the problem of dike's stability, since most of the country is below sea level and it is protected from flooding by a complex system of dikes. A way to improve dike's stability is the implementation of a low permeable layer below the dike, in order to reduce the seepage. The SoSEAL project is born in order to find out a cost effective and environmental friendly technology, that is able to reduce soil permeability. The idea of the SoSEAL project is to inject in the subsurface a suspension of aluminium (Al) and organic matter (OM). The interaction between aluminium and organic matter leads to the precipitation of metal-OM complexes that reduce soil permeability.

Studies have been conducted so far to develop the technology, but there are still many unanswered questions to be solved. One of those is about the mobility of Al-OM flocs in porous media and this research is meant to obtain a better knowledge about it. The aim of this project is to enhance this technology under controlled laboratory conditions and in particular to define the injection conditions that ensure a relevant precipitation of Al-OM flocs and thus a relevant hydraulic conductivity reduction. The hydraulic conductivity reduction should be distributed homogeneously along the column, so that, in the field, it would be possible to build a large area of low hydraulic conductivity. Different column experiments have been performed, in order to determine a relation between the injection flow rate and the hydraulic conductivity reduction that can be achieved along the column. In addition, the effect of the change of the injection flow rate on Al-OM floc mobility has also been investigated. The sand, the packing, and the suspension used are always kept constant. The only parameter that has been changed during the experiments is the flow rate.

The results show that the increase in the flow rate implies an increase in the Al-OM floc transport along the column, with an increase in the mass collected in the outflow. The highest hydraulic conductivity reduction is in the first 5 cm of the column, up to 300 times, while in the rest of the column it is below 40 times, with a total hydraulic conductivity reduction that is around 100 times. Therefore, a relevant hydraulic conductivity reduction has been reached, that could strongly enhance the soil characteristics. However, it is still necessary to improve the technology, in order to obtain a higher radius of influence and a larger area of low hydraulic conductivity.

Riassunto

I Paesi Bassi si trovano ad affrontare il problema della stabilità delle dighe, dal momento che la maggior parte della regione è al di sotto del livello del mare ed è protetta dal rischio di inondazioni da un complesso sistema di dighe. Una tecnica per il miglioramento della stabilità delle dighe consiste nella realizzazione di uno strato a bassa permeabilità sotto la diga, al fine di ridurre le infiltrazioni. Il progetto SoSEAL nasce per individuare una tecnologia a basso costo e impatto ambientale, in grado di ridurre la permeabilità del suolo. L'idea di questo progetto è di iniettare nel suolo una sospensione di alluminio (Al) e materia organica (OM). L'interazione tra l'alluminio e la materia organica porta alla precipitazione di complessi metallo- materia organica, i quali riducono la permeabilità del suolo.

Diversi studi sono stati effettuati finora per sviluppare tale tecnologia, ma sono presenti alcuni interrogativi ancora da risolvere. Uno di questi riguarda la mobilità degli aggregati di Al-OM nel mezzo poroso, per cui, questa ricerca mira a ottenerne una migliore conoscenza. L'obiettivo di questo progetto è ottimizzare questa tecnologia in condizioni controllate di laboratorio e in particolare definire quali condizioni di iniezione garantiscono una deposizione significativa di aggregati di Al-OM e, conseguentemente, una significativa riduzione di conducibilità idraulica. Si vuole ottenere una riduzione di conducibilità idraulica distribuita in modo più omogeneo possibile lungo la colonna, in quanto questo permetterebbe la creazione, in campo, di una zona a bassa conducibilità idraulica più estesa. Diversi esperimenti in colonna sono stati realizzati, al fine di determinare una relazione tra la portata di iniezione e la riduzione di conducibilità idraulica che può essere ottenuta lungo la colonna. Inoltre, si è anche voluto investigare l'effetto del cambiamento della portata di iniezione sulla mobilità dei flocculi di alluminio e materia organica. La sabbia utilizzata, la preparazione della colonna e la sospensione iniettata sono tenuti costanti durante ogni prova. L'unico parametro che viene modificato è la portata di iniezione.

I risultati mostrano che l'aumento della portata implica un aumento del trasporto dei flocculi di alluminio e materia organica lungo la colonna, con l'aumento della massa raccolta all'uscita della colonna. La maggiore riduzione di conducibilità idraulica si riscontra nei primi 5 cm della colonna, dove si ha una diminuzione di 300 volte rispetto al valore iniziale, mentre nel resto della colonna tale riduzione è al di sotto di 40 volte, con un valore complessivo lungo tutta la colonna di circa 100. Di conseguenza, è stata ottenuta un'elevata riduzione di conducibilità idraulica, la quale permetterebbe un netto miglioramento delle caratteristiche del suolo. Tuttavia è necessario sviluppare ulteriormente la tecnologia, in modo da estendere la zona influenzata dall'effetto di riduzione di conducibilità idraulica.

Contents

List of Figures

List of Tables

Abbreviations

CFT Clean bed Filtration Theory;

DOM Dissolved Organic Matter;

EC Electrical Conductivity;

HCR Hydraulic Conductivity Reduction;

M/C Metal Carbon ratio;

NOM Natural Organic Matter;

OM Organic Matter;

PV Pore Volume;

TOC Total Organic Carbon;

SoSEAL Soil Sealing by Enhanced Aluminium and DOM Leaching;

Chapter 1

Introduction

The issue of dike's stability is strongly important in the Netherlands, where the 60% of the total population lives in low-lying areas and flood protection measures have to provide safety for the inhabitants (Pilarczyk, 1998). The reduction of soil permeability is a fundamental improvement for dike's stability (Xu, 2013), since a common problem connected to dikes is the seepage through high permeable layers underneath the dike. The seepage influences the global stability (Benmebarek, Benmebarek, & Kastner, 2005) because it leads to the detachment of particles from the soil matrix inside the dike and to internal erosion, which deteriorates the soil structure (Danka & Zhang, 2015). However, many of the existing techniques to lower soil permeability require substantial energy for material production or installation and are expensive (DeJong, Mortensen, Martinez, & Nelson, 2010), when considering that hundreds of kilometres of dike stretches need to be tackled to protect inhabitants from flooding (de Moel, Bouwer, & Aerts, 2014). For this reason, the Netherlands is looking for new technologies to reduce permeability in an environmental friendly and cost effective way.

Therefore, SoSEAL project is meant to develop a new bio-based geo-engineering technology to reduce permeability in the subsurface. SoSEAL is an acronym for Soil Sealing by Enhanced Aluminium and DOM Leaching. The concept is to create less permeable layers by the precipitation of aluminium and dissolved organic matter (DOM) (Zhou, Laumann, & Heimovaaraa, 2019). Aluminium and organic matter interact with each other and create flocs, that tend to precipitate. These precipitates clog the pore space and thus reduce permeability.

The idea for the SoSEAL project arises from a natural process called podzolization. This phenomenon is typical of coniferous forests, where it is possible to find layers of low permeability formed by metal-organic matter precipitates (Sauer, Sponagel, Sommer, Giani, Jahn, & Stahr, 2007). The podzolization process is based on the reaction between OM and Al and Fe to form organic-metal complexes. OM is naturally present in the upper horizon of the soil and it leaches downward, where there is an high amount of Fe and Al. The bindings between OM and Al and Fe lead to the precipitation of Al/Fe complexes. The accumulation of these complexes results in permeability reduction (Lundstrom, Van Breemen, & Bain, 2000).

The permeability reduction can be achieved in two ways: on the one hand it can be obtained through the gradual and complete filling of the pore space; on the other hand it can be achieved through the clogging of the pore throat (Sharma & Yortsos, 1987). The size of Al-OM flocs is around hundreds of micrometres (Wang, Gao, Xu, Xu, & Xu, 2009), thus the most probable mechanism to reduce permeability can be connected to the clogging of the pore throat instead of the filling of the pores (Sharma & Yortsos, 1987). This mechanism can strongly increase the efficiency in reducing permeability, because this would imply the necessity of less mass to obtain a high permeability reduction. For this reason, the development of this technology can be really interesting, since the capacity to reduce the permeability in a cost effective way can be remarkable in several respects. It could be useful to improve dike's stability, but also to prevent the spreading of contaminants in a polluted site or below landfills (Mulligan, Yong, & Gibbs, 2001).

1.1 Previous results of SoSEAL project

Starting from the analysis of the podzolization process, many studies have been performed within the SoSEAL project so far. In particular, this technique has been applied to two field experiments. In the first field experiment, Al and OM were injected separated in a cylindrical conformation, in order to obtain a vertical flow barrier in a sand layer at depth (Zhou, Laumann, & Heimovaaraa, 2019). The results show that the precipitation was a highly localized process and the large amount of precipitates was formed near the injection point. In addition, the barrier was shifted towards the downstream direction. However, the in situ production of Al-OM was able to reduce the permeability up to 2%. The quantification of the permeability reduction was a challenge, because it was not possible to exactly determine the spatial distribution of Al-OM precipitates, which would have been the interpretation key of field measurements. Moreover, not all the material injected reacts to form Al-OM flocs and to create the barrier, thus the in situ mixing is not very efficient (Zhou, Laumann, & Heimovaaraa, 2019). According to those results, it has been decided to proceed the research towards the injection of Al-OM suspension and the investigation of floc mobility.

The injection of Al-OM suspension implies the production of Al-OM flocs ex-situ and a better control of the reaction that takes place. The direct injection of the suspension is feasible because floc size is decreased under high shear condition (Li, Zhu, Wang, Yao, & Tang, 2006). The shear stress is caused by the force applied parallel to the cross-section of the material. During the field test, different compartments of shear can be distinguished: the vessel, where the Al-OM suspension is continuously stirred, the pipes, the pump, the injection point, where there is the highest shear stress, and the soil, where the suspension bumps over soil particles. Therefore, due to high shear conditions, Al-OM flocs are small enough to be transported through porous media. However, when low-shear conditions prevail, the Al-OM flocs re-grow in size and block the pore space with a reduction in permeability (Jarvis, Jefferson, & Parsons, 2005). The feasibility of the direct injection has been verified both in laboratory experiments and in the second field experiment (Zhou, Laumann, & Heimovaaraa, in progress).

1.2 Research goals

The question about floc mobility in porous media is still unanswered. For this reason, in this research, the mobility of Al-OM flocs and their potential to reduce the permeability of Al-OM flocs will be investigated. The main goals are as follows:

- First of all it is necessary to determine the injection rate that distributes the Al-OM flocs homogeneously along the column. This ideal situation requires that the flocs are small enough to flow through the column, but at the same time able to regrow and reduce permeability.

- The second step is to evaluate permeability reduction due to the presence of flocs in the column.

In order to answer those questions, column experiments are prepared, in which the Al-OM suspension is injected at different flow rates. Pressure sensors along the column allow to determine the variation of pressure during the injection and thus to calculate the hydraulic conductivity reduction in each section of the column.

1.3 Hypothesis

Before performing the experiments, a hypothesis regarding the most likely results can be made. Considering the distribution of flocs in porous media, it is expected that most of the injected mass will remain near the inlet, while the rest of the column will not be affected by the presence of flocs (Bradford, Yates, Bettahar, & Simunek, 2002). When flocs enter into the porous medium an hydraulic conductivity reduction (HCR) is expected, since they clog the pore space (Costa, 2006). The hydraulic conductivity reduction is defined as the ratio between the initial hydraulic conductivity during water injection, K_0, and the hydraulic conductivity measured at the end of the injection of Al-OM flocs, K:

$$HCR = \frac{K_0}{K} \quad (1.1)$$

Therefore, considering that most of the injected mass will remain near the inlet, also the highest HCR is expected at the column inlet (Costa, 2006).

However, the ideal situation would be to obtain a homogeneous distribution of flocs along the column and a constant HCR. It is very unlikely to reach this ideal situation, nevertheless, the aim is to obtain the most homogeneous distribution possible. Thus, the desired situation is to observe the highest HCR in the first part of the column, but still a significant HCR along the whole column.

A representation of the expected distribution on HCR is shown in Figure 1.1

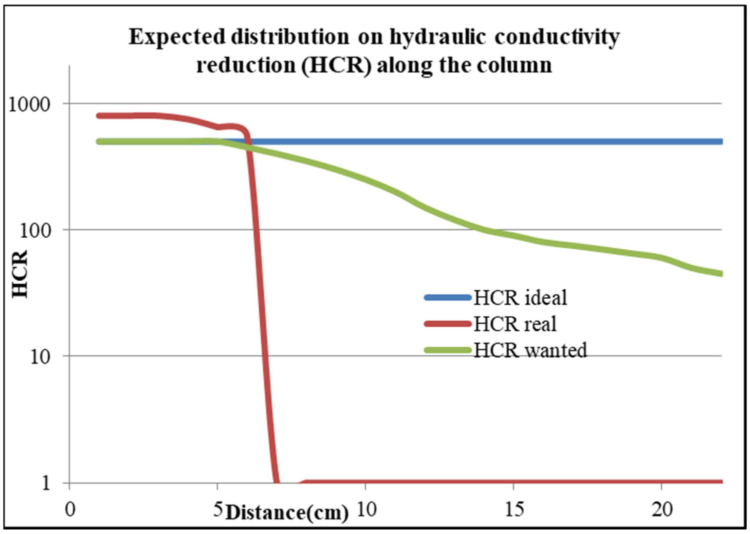

Figure 1.1: Presentation of the possible distributions on hydraulic conductivity reduction along the column.

In Figure 1.1, the blue line shows the ideal situation, in which a homogeneous floc distribution and a constant HCR is present along the whole column. On the contrary, the red line shows the more realistic situation, in which all flocs are filtered in the first 6 cm of the column. The wish is to obtain something in between those two situations, as shown by the green line. In this circumstance, the highest HCR is in the first part of the column, but there is still a significant reduction also in the rest of the column.

Chapter 2

Theoretical Background

Soil permeability is the property of the soil to transmit water and it depends on soil texture and porosity (Di Molfetta & Sethi, 2012). The injection of Al-OM flocs in porous media can reduce soil permeability because of Al-OM precipitation that clogs pores (Zhou, Laumann, & Heimovaaraa, 2019). For this reason, it is important to study Al-OM interactions, in order to find out in which conditions they form flocs and which phenomena could affect them. Another important element that must be considered is the regrowth of flocs after shear stress, because the injection method implies that flocs are subject to shear rate, which could strongly affect the dimension of flocs.

Finally, it is necessary to analyse general transport phenomena in porous media, such as advection and dispersion, but also particle-particle and particle-porous medium interactions, such as DLVO and colloidal filtration theory, blocking and ripening. In this way, it is possible to better understand which kind of phenomena can affect the mobility of flocs.

2.1 Al-OM interaction

Aluminium in solution can be present in different forms, according to pH (Duan & Gregory, 2003), as shown in Figure 2.1.

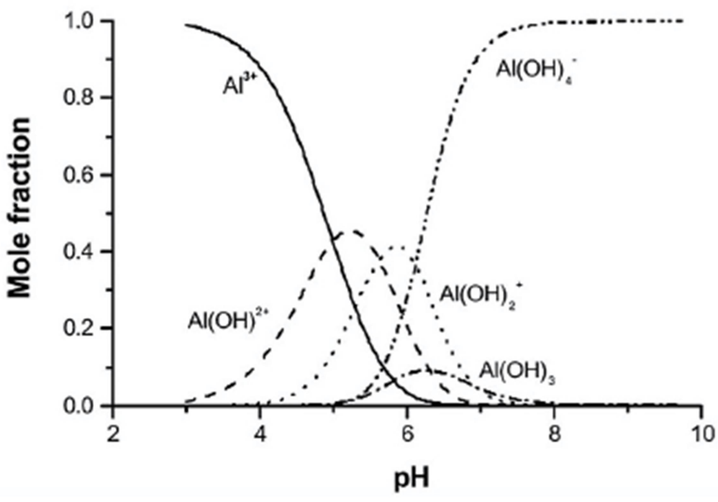

Figure 2.1: Mole fractions of dissolved hydrolysis products in equilibrium with amorphous hydroxide (Duan & Gregory, 2003)

Figure 2.1 presents the aluminium speciation at different pH. The ability of aluminium to complex with organic matter is strongly connected with aluminium speciation, thus it is also connected with pH. Aluminium can be present in an acidic solution as free ion or as mono-hydroxide and di-hydroxide ions, which have a decreasing positive charge and thus different capacities to interact with organic matter (Nierop, Jansen, & Verstraten, 2002). The form with the highest positive charge, Al^{3+}, is the one able to create the most binding sites with OM and it is generally present at low pH, below 5 (Hagvall, Persson, & Karlsson, 2015).

Organic matter is able to form rigid structures with aluminium because of carboxylic and phenolic groups, which are the most important functional groups of OM. Those functional groups are deprotonated at low pH, therefore, they are able to form more bindings with Al (Hagvall, Persson, & Karlsson, 2015). Thus, pH is a relevant parameter able to influence floc formation. When pH is below 5 and Al and OM are in solution, complexation is very fast and it results in the precipitation of insoluble flocs, which can reach a diameter of hundreds of micrometres.

The organic matter that is generally used in this process is the humic acid and there are two main mechanisms for the precipitation of humic substances by metal coagulants:

- Binding of metal species to anionic sites. It implies the charge neutralization between aluminium and organic matter and so a reduced solubility and precipitation;
- Adsorption of humic substances on metal hydroxide precipitate. At pH values around 6, the aluminium hydroxides are positively charged while humic substances are negatively charged, thus, strong adsorption and some charge neutralisation are expected.

However, generally, it is not easy to distinguish between those two mechanisms (Duan & Gregory, 2003). Nevertheless, a general consideration that can be deduced is that at a pH value higher than 6 the removal of OM is supposed to be dominated by adsorption onto precipitated metal hydroxides. On the other hand, at pH below 6 the main removal mechanism is assumed to be the complexation of OM with soluble metal species into insoluble precipitates (Jarvis, Jefferson, & Parsons, 2006).

Traditionally, when OM precipitates through a combination of charge neutralization and complexation with coagulant metal hydrolysis, flocs are considered weak and fragile. Instead, if OM is removed through adsorption onto metal hydroxide precipitates, the strength of the flocs is derived from a combination of organic interactions, such as steric and bridging mechanisms, and electrostatic forces (Sharp, Jarvis, Parsons, & Jefferson, 2006).

Floc strength is an important parameter that is connected to floc structure and formation process. It can be defined as the energy required to break flocs under tension, compression or shear, or as the size that flocs reach at the end of the growth phase. Floc strength generally increases with a decrease in floc size, because of floc compaction and the number of internal bounds. However, it is difficult to measure this parameter, because of the fragility and complexity of floc structure (Jarvis, Jefferson, Gregory, & Parsons, 2005).

A schematic representation of floc formation is presented in Figure 2.2.

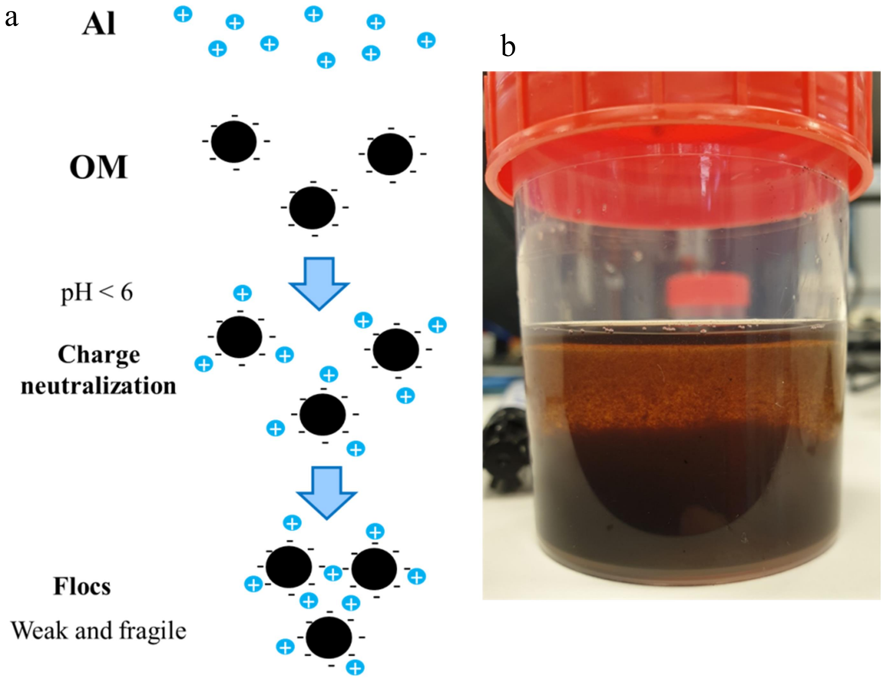

Figure 2.2: Schematic representation of Al-OM floc interaction (a) and picture of the Al-OM flocs with the OM concentration of 1 g/l and a M/C ratio of 0.03 (b)

2.2 Effect of pH, M/C ratio and shear rate

Size and stability of flocs depend on different external conditions, such as pH, metal-carbon ratio and shear rate. These parameters must be considered when working with Al-OM flocs, because they can affect floc dimension and formation and therefore floc mobility. They have been analysed in different studies for wastewater treatment and also during SoSEAL project.

2.2.1 The effect of pH

As seen in the previous paragraph, pH can modify floc formation and size because it determines both the degree of dissociation of the acidic functional groups on the organic molecules and the inorganic speciation of metals that can bind to organic matter (Jansen, 2003). Increased pH implies a decrease in the available binding sites and thus in floc size, because of aluminium speciation and OM functional groups. On the one hand, Al^{3+} is present at pH below 5, while at higher pH mono- and di-hydroxide ions forms are present that are less capable to interact with OM. On the other hand, with increasing pH, OM protonation takes place and less functional groups will be able to bind with aluminium (Jansen, 2003; Hagvall, Persson, & Karlsson, 2015; Hopman, 2016). Therefore, a low pH allows to obtain more binding sites, bigger flocs and thus a faster precipitation of Al-OM flocs, as possible to observe in Figure 2.3.

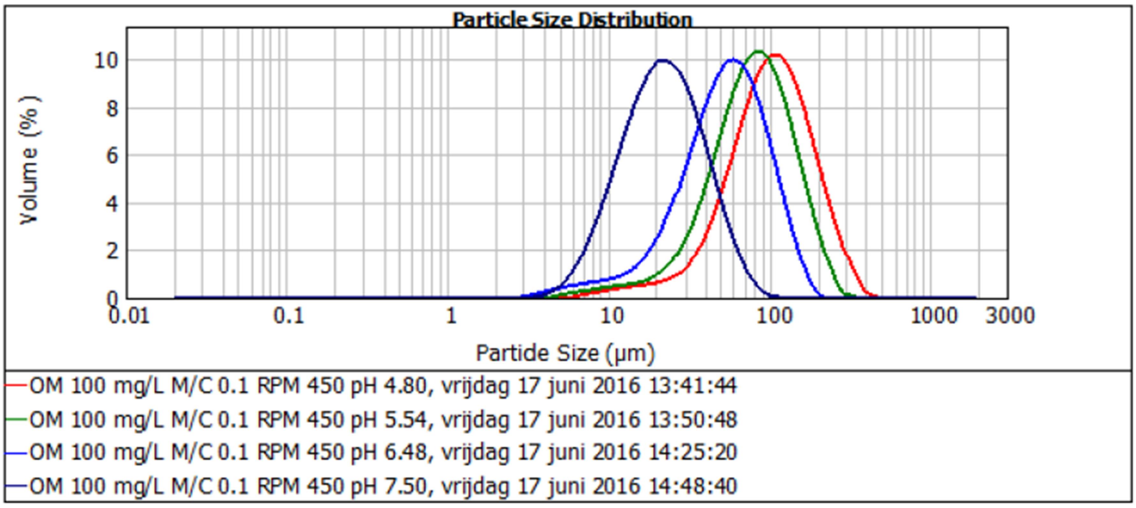

Figure 2.3: Particle size distribution for different pH values at a fixed shear rate. (Hopman, 2016)

Figure 2.3 presents the particle size distribution for different pH. The suspension used and the shear rate applied are kept constant, while the pH is changed. As possible to notice, with the decrease in the pH, the Al-OM precipitates are bigger, since Al^{3+} can bind more OM molecules (Hopman, 2016).

However, decreasing the pH has not always the effect of increasing floc size. It is possible to obtain bigger flocs at a pH around 4.5 than at lower pH (Scheel, Haumaier, Ellerbrock, Rühlmann, & Kalbitz, 2008). If the acidity of the system is too high, the organic polyelectrolytes are less soluble, because of the protonation of organic functional groups. In addition, a decrease in the pH means an increase in the H^+, which compete with metals for organic binding sites. Thus, it is possible to observe a decrease in the overall extent of metal-induced flocculation and precipitation of OM (Kleber, Eusterhues, Keiluweitk, Mikutta, Mikutta, & Nico, 2015). Therefore, the optimum value of pH for high floc size and precipitation is an intermediate value between 4 and 5.

2.2.2 The effect of M/C ratio

The metal-carbon ratio takes into account the amount of aluminium that must be added to the OM solution, in order to obtain Al-OM flocculation. There is an optimum value of M/C ratio at which precipitation occurs and the size of precipitated flocs is the highest (Zhou, Laumann, & Heimovaaraa, 2019). When aluminium is added to the OM solution, aluminium ions react and bind with OM. The binding between Al and OM results in the formation of flocs that precipitate. After the saturation of the bindings present on OM molecules, if aluminium chloride hexahydrate solution is still added, it will only result in more free ions. This increase in free ions implies an increase in electrostatic repulsion by residual positive charge left on Al cations that are already bound to organic matter (Jansen, 2003; Kleber, Eusterhues, Keiluweitk, Mikutta, Mikutta, & Nico, 2015; Hopman, 2016). Thus, a decrease in particle size and in precipitation can be observed. For this reason, it is necessary to find out which is the amount of aluminium that must be added to obtain precipitation, without increasing the electrostatic repulsion. In this way, it is possible to obtain the biggest flocs and the minimum dispersion of free aluminium in the environment.

2.2.3 The effect of the shear rate

Shear rate is a parameter that strongly influences floc size. Floc dimension decreases with the increase in shear rate, since it influences the stability of flocs.

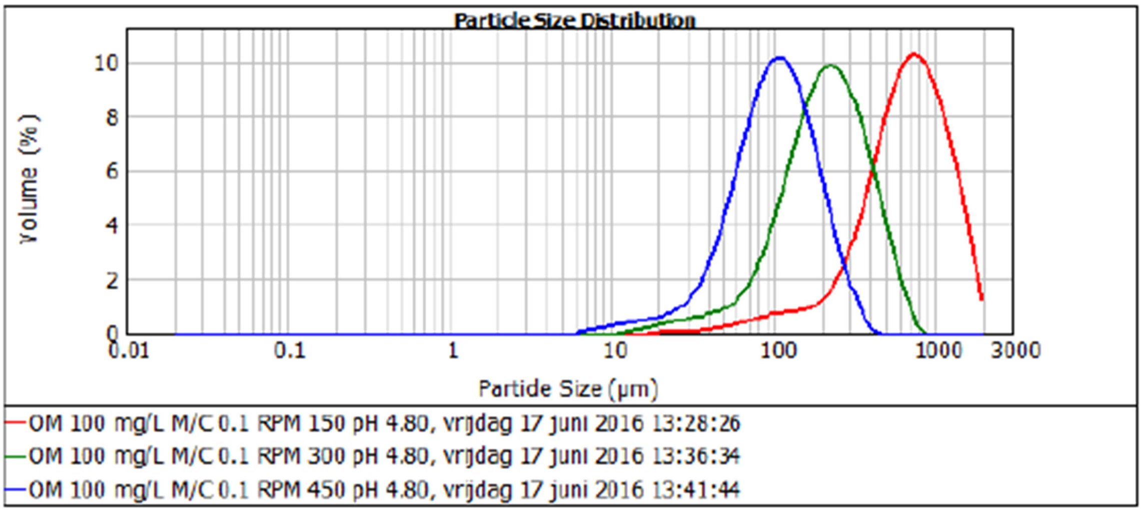

Figure 2.4: Particle size distribution for different shear rate at pH 4.80 (Hopman, 2016)

Figure 2.4 shows the decrease in particle size with the increase in the shear rate at which they have been subject. In general, at the beginning of high shear rate application, there is an immediate decline in floc size, while for low shear rate this decline is less relevant (Jarvis, Jefferson, & Parsons, 2006). Thus, the reduction of floc dimension is much more affected by a high shear rate, than by a low one. After a certain time of exposure to shear rate, the floc aggregates approach a steady-state floc size after which no further significant degradation in floc size is seen, so there is a minimum stable size (Jarvis, Jefferson, & Parsons, 2006).

Shear rate at which flocs are subject is also a fundamental parameter to evaluate their re-growth. When flocs are subject to shear rate, their dimension decreases and, only when a low- or no- shear rate condition is restored, there is the possibility for flocs to re-grow till a certain dimension, that depends on the shear rate at which they have been subject. In particular, when flocs are exposed to high shear for a sustained period, such as 15 minutes, floc re-growth is limited and they are not able to reach their previous size (Jarvis, Jefferson, & Parsons, 2005).

On the contrary, when flocs are exposed to a short period of high shear, the extent of floc breakage is much less and flocs are able to re-grow to a size closer to their previous one. Thus, sustained exposure to high shear will break flocs with little re-growth capacity (Jarvis, Jefferson, & Parsons, 2005). Floc suspensions have a much better capability to reach their previous size when only exposed to short periods of high shear (Jarvis, Jefferson, & Parsons, 2006), as presented in Figure 2.5.

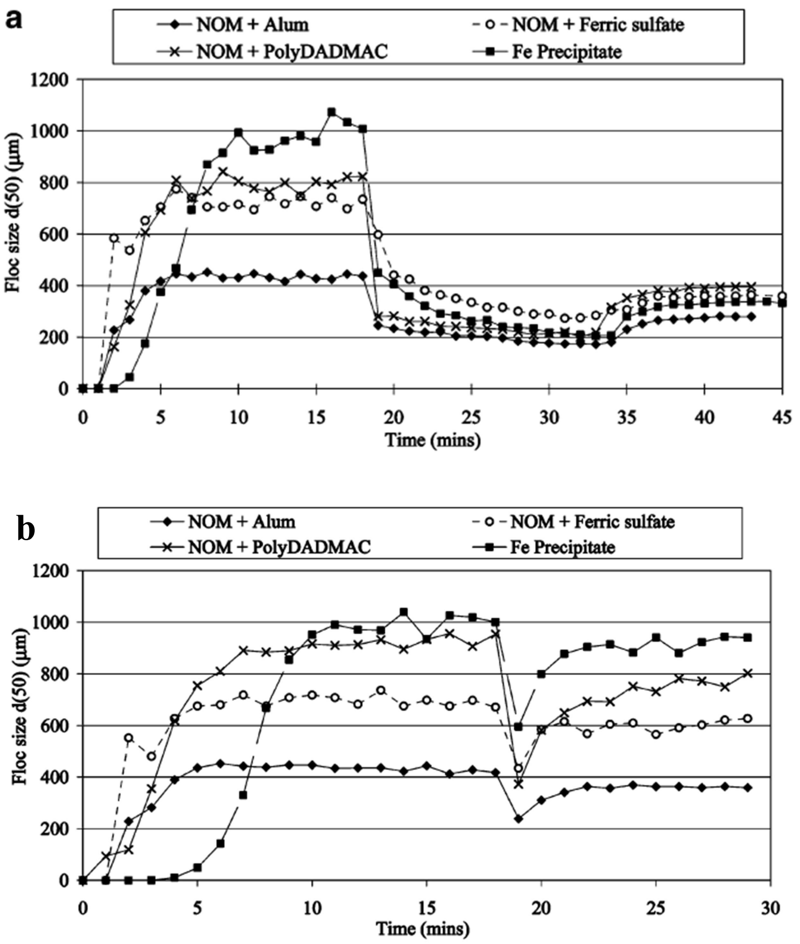

Figure 2.5: Breakage and regrowth profile of NOM flocs formed from three different coagulants. At first a rapid mixing at 200 rpm for 1.5 min, then a low stir phase at 30 rpm for 15 minutes, followed by a breakage phase at 200 rpm. Two separate breakage periods are investigated: a long shear period of 15 minutes (a) and short shear period of 30 seconds (b). Finally a slow stir phase at 30 rpm for 15 minutes, to observe floc regrowth (Jarvis, Jefferson, & Parsons, 2005)

As possible to observe in Figure 2.5, Al-OM flocs that have been subject to high shear period are not able to regrow to the same size as the ones that have been subject to low shear period, even though the size reached during the breakage period is almost the same.

Floc regrowth is also connected to the phenomena arisen during their formation. Three coagulation mechanisms may occur:

- Charge neutralization is the process for which the negative charge, present on organic matter, is neutralized by the addition of low concentration metal coagulants. There is an optimum dosage over which particles become positive charged and don't aggregate anymore.

- Sweep flocculation occurs when metal coagulants are added at dosages much higher than the one used for charge neutralization. The original particles are incorporated into the growing hydroxide precipitate and are removed from suspension. Sweep flocculation leads to faster aggregation than charge neutralization and gives stronger and larger flocs.
- Bridging flocculation occurs when an adsorbing polymer is added to a suspension of particles, and so a single chain may become attached to two or more particles. Those aggregates are stronger than all the previous ones (Gregory, 2006).

Those coagulation mechanisms affect the strength and the dimension of the final flocs, but also their ability to regrow. Flocs formed through bridging or sweep flocculation, generally, are not able to regrow (Li, Zhu, Wang, Yao, & Tang, 2006). Since the ability of flocs to regrow allows an improvement of permeability reduction, the main coagulation mechanism, for the suspension used in this project, is charge neutralization.

During field and column experiments, the shear rate at which flocs are subject is mainly determined by the flow rate of injection, therefore it is a relevant parameter that must be taken into account. It is expected that an increase in the flow rate would allow a higher mobility of flocs. If the flow rate of injection is high, flocs are subject to a high shear rate which decreases floc size. This would mean that they are more mobile and can be transported further along the column. On the contrary, if the flow rate is low, flocs are subjected to a low shear rate and are bigger and less mobile (Jarvis, Jefferson, & Parsons, 2006).

However, if the shear rate is too high, it can destroy the flocs to such a small size that they are not able to regrow anymore (Yu, Gregory, & Campos, 2010). If flocs are too small, they are not able anymore to reduce the hydraulic conductivity. Thus, it is important to discover an optimal flow rate that allows the Al-OM flocs to be mobile but also keep their potential to reduce the hydraulic conductivity.

2.3 Hydraulic conductivity reduction

The aim of this study is to inject flocs in a porous medium, in order to reduce the hydraulic conductivity. The hydraulic conductivity is the volumetric flow of water that flows through a porous medium per unit cross section under the effect of a hydraulic gradient of unit value at 20ºC (Di Molfetta & Sethi, 2012). It can represent the ability of the fluid to pass through the pores and it depends on porous media features and on fluid. It is generally defined by Darcy law:

$$Q = KA\frac{\Delta h}{L} \quad (2.1)$$

Where Q is the flow rate (m^3/s), K is the hydraulic conductivity (m/s), A is the area perpendicular to the flow (m^2), $\Delta h/L$ represents the hydraulic gradient.

Permeability, k, is a porous media intrinsic property and it is connected to hydraulic conductivity with the following formula:

$$K = g\rho\frac{k}{\mu} \quad (2.2)$$

Where K is the hydraulic conductivity (m/s), g is the gravity acceleration (m/s^2), ρ is the density of the fluid (kg/m^3), k is the permeability of the porous medium (m^2) and μ is the dynamic viscosity of the fluid (kg/ms). Thus, permeability and hydraulic conductivity are linearly correlated, so only hydraulic conductivity reduction will be evaluated (Fitts, 2013).

During column experiments, it is possible to measure the difference of pressure along the column, that allows to calculate the hydraulic conductivity with the relationship:

$$K = \frac{Q}{A}\frac{H}{\Delta P} \quad (2.3)$$

Where Q is the flow rate of the solutions through the column (m^3/s), A is the area perpendicular to the flow (m^2), H is the height of the column and ΔP (m) is the pressure drop measured by sensors (Di Molfetta & Sethi, 2012).

The knowledge of the hydraulic conductivity before and after floc injection makes it possible to evaluate hydraulic conductivity reduction, that is calculated as:

$$HCR = \frac{K_0}{K} \quad (2.4)$$

Where K_0 is the hydraulic conductivity obtained during the injection of water, while K is the hydraulic conductivity that is measured in any point of the injection. So the HCR is expressed in how many times the hydraulic conductivity has been reduced compared to the initial hydraulic conductivity.

2.3.1 Kozeny-Carman equation

The HCR can be achieved due to the presence of flocs into the porous media, because they reduce pore space. For this reason, it is necessary to analyse the relationship between porosity and permeability, that is explained by the Kozeny-Carman equation.

The Kozeny–Carman equation relates the pressure gradient and flow rate for fluid that flows through porous media. It is applicable to unconsolidated packed media, composed of spherical particles. Kozeny considered a porous medium as an assembly of capillaries of specific size and geometry with fluid flow through them. Then, Carman modified the equation taking into account the fact that fluid flow through the voids of a porous media is tortuous (Tien & Ramarao, 2013).

Thus, the Kozeny-Carman model is able to figure out a relationship between porous media properties and flow resistance in pore channels.

It is an attempt to describe permeability in terms of porosity, with the following formulation:

$$k = C_{kc} \frac{n^3}{(1-n)^2} \quad (2.5)$$

Where k is the permeability, n is the porosity and C_{kc} is a parameter that takes into account the internal surface area and the tortuosity (Costa, 2006).

According to the equation 2.5, it is possible to calculate the porosity that should have been obtained in the porous medium after floc injection, since the initial porosity and the initial and final permeability are measured during column experiments.

Another way to calculate the porosity after floc injection consists in the evaluation of the variation of the pore volume due to the amount of injected flocs. It is possible to estimate the porosity after floc injection as follows:

$$n_i = \frac{PV - V_f}{V_{tot}} \quad (2.6)$$

Where the PV is the pore volume calculated during the tracer test, V_f is the volume of flocs that has been injected in the column, and V_{tot} is the total volume of the column. The volume of flocs has been calculated as the ratio between the injected mass and the floc density, which is considered as water density. In this way, the porosity after the injection, n_i, can be estimated.

Therefore, a comparison between the porosity calculated with the Kozeny-Carman equation and with the equation (2.6) allows to evaluate if the Kozeny-Carman equation is suitable to model the process that occurs in the porous media with floc injection. Two main processes can lead to permeability reduction: the complete filling of the pore space or the clogging of the pore throat (Sharma & Yortsos, 1987), as shown in Figure 2.6

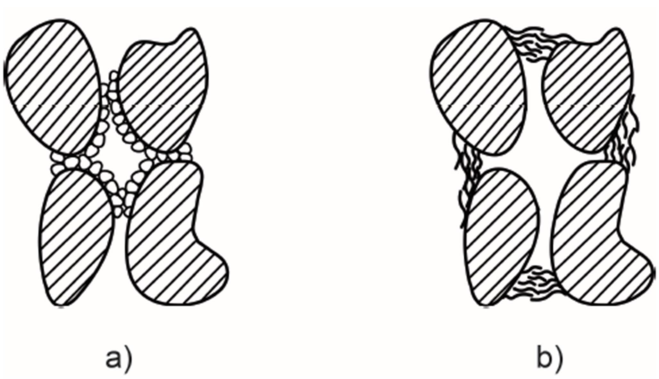

Figure 2.6: Comparison between the behaviour of particles that fill the pore space and particles that clog the pore throat (Bonfiglio, 2017)

In Figure 2.6, the mechanisms of pore filling, Figure 2.6 a, and of clogging of the pore throat, Figure 2.6 b, are presented. When particles are able to clog the pore throat, the amount of particles necessary to obtain a relevant reduction in hydraulic conductivity is less than the amount necessary to fill the pore space and to obtain the same reduction (Sharma & Yortsos, 1987).

2.4 Transport in porous media

Transport of solutes in porous media is, generally, ruled by two main mechanisms: advection and dispersion. Advection is connected to water flow into porous media and, in laminar groundwater flow, it causes only longitudinal spreading. On the contrary, dispersion is responsible of the lateral spreading of the solute and it is the sum of the molecular diffusion and kinematic dispersion (Logan, 2001). The molecular diffusion is a mixing that occurs because of the random motion of molecules in a fluid and it moves solute from the regions at high concentration towards the ones at low concentration. The kinetic dispersion, instead, is connected to velocity variation and porous medium heterogeneity (Fitts, 2013).

If solutes are reactive, it could be necessary also to evaluate sorption and biodegradation. Sorption is an interaction between solute and porous media, that generally brings to a retardation in solute transport. Biodegradation, instead, is the decrease in solute concentration due to the presence of bacteria that are able to degrade them into other species (Di Molfetta & Sethi, 2012; Fitts, 2013).

Those mechanisms are generally present when considering a solute transport. However, when considering particles transport in porous media, it is necessary to take into account their interaction with porous media. Thus, it is also necessary to analyse the collision and DLVO theory and the Clean Bed Filtration Theory.

2.4.1 Collision and Attachment in DLVO Theory

The injection of Al-OM flocs implies a colloidal suspension, which is subject to both chemical and physical forces. This means that it is important to evaluate also particle-porous media interaction and particle particle-interaction. When particles are injected in a porous medium, they can collide with its grains thanks to gravity or interception for big particles, or Brownian motion for submicron particles (Tufenkji & Elimelech, 2004). After collision, particles can attach to grain according to chemical forces. Attachment has been defined in DLVO (Derjaudin, Landau, Verwey, Overbeek) theory as the sum of electrostatic and Van der Waals forces (Ryan & Elimelech, 1995).

The electrostatic force is repulsive because of the negative charge generally present both on particles and porous media grains. The magnitude of repulsion between similarly charged surfaces depends on the size of the interacting particles, the distance of separation, the surface potential of particles and collectors, and the electrolyte concentration (Elimeiech & O'Meila, 1990). Repulsion is stronger at short distances between particles and grain and then it decreases as an exponential. However, the increase in the ionic strength present in solution can decrease repulsion because of charge neutralization (Tosco, Bosch, Meckenstock, & Sethi, 2012).

For what concerns Van der Waals forces, they are attractive and they depend on the size of the interacting particles, the distance of separation between particles and collector, and the Hamaker constant of the interacting media (Elimeiech & O'Meila, 1990). In particular, they are stronger at small distances, but they decrease faster than electrostatic forces. Therefore, the combination of those two forces can give different results, which decide if attachment can occur or not. The potential energy diagram, presented in Figure 2.7, shows the contribution of both effect.

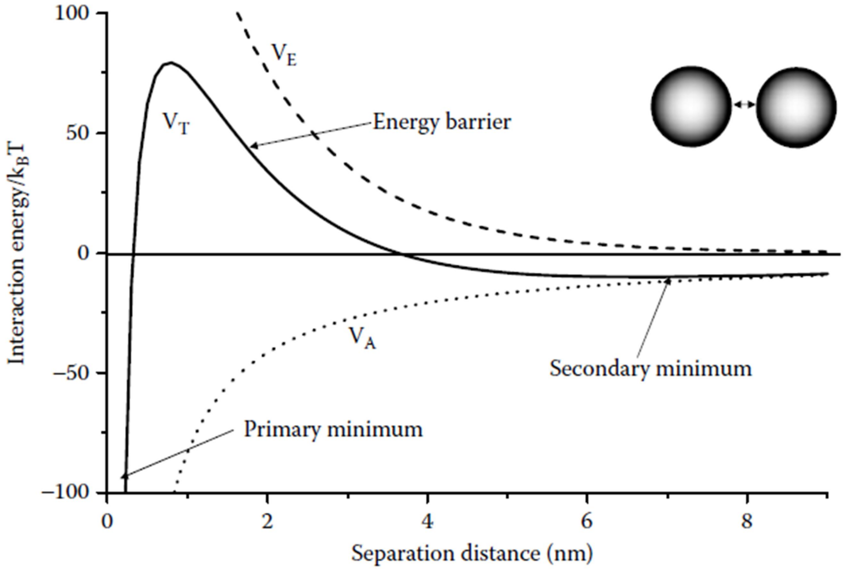

Figure 2.7: Potential energy diagram (Gregory, 2006)

In Figure 2.7, it is possible to observe the contribution of the electrostatic energy, V_E, which is represented by an exponential decrease with the increase in the distance, the van der Waals interaction energy, illustrated by V_A, and the total interaction energy, represented by V_T, which is the sum of both contribution. At small distance, the van der Waals force prevails, therefore, there is the primary minimum and the particles tend to attach. At large distance too, the attraction term is higher than the repulsion, because the electrostatic energy presents an exponential decrease with distance, while the van der Waals attraction varies inversely with distance (Gregory, 2006). For this reason, there is the secondary minimum. Between those two minimums, instead, the repulsion prevails, forming an energy barrier that prevents attachment.

In the presented situation, it is extremely unlikely that particles would be able to overcome the energy barrier, because the repulsive force prevails on the attractive force. Thus, the attachment is improbable in this configuration. However, it is possible to decrease the repulsive electrostatic force and, consequently, to compress the energy barrier by increasing the ionic strength present in solution. As the ionic strength is increased, the diffuse layer becomes thinner and particles can approach closer before feeling any repulsion (Gregory, 2006). On the contrary, for a specific ionic strength, it is possible to observe a decrease in the attachment when the flow rate is increased, because the increase in the flow rate causes the extension of the double layer thickness (Mesticou, Kacem, & Dubujet, 2016). According to these considerations, different configurations can be present in a system and they can decide if the attachment prevails or not.

In summary, the deposition rate of particles can be seen as a product of an attachment efficiency and a dimensionless transport rate (Elimeiech & O'Meila, 1990). The attachment efficiency considers chemical colloidal effects on the rate of deposition, while the transport rate takes into account physical collision effects. When chemical-colloidal interactions are favourable for deposition the attachment efficiency approaches unity, and the deposition rate is equal to the transport rate (Gregory, 2006).

2.4.2 Clean Bed Filtration Theory

The Clean Bed Filtation Theory (CFT) describes nano and micro particles transport in porous media and attempts to evaluate deposition kinetic with attachment efficiency and single-collector contact efficiency. The single-collector contact efficiency describes the transport of particles to a collector as the cumulative effect of diffusion (η_D), interception (η_I), and gravitational sedimentation (η_G), and it can be calculated as follows (Laumann, Vesna, Lowry, & Hofmann, 2013):

$$\eta_0 = \eta_D + \eta_I + \eta_G \quad (2.7)$$

This formula can also be expressed as:

$$\eta_0 = 4.04{A_s}^{1/3} N_{Pe}^{-2/3} + \frac{3}{2} A_s N_R^2 + N_G \quad (2.8)$$

Where A_s is the variable depending on porosity, N_{Pe} is the Peclet number, N_R is the steric number and N_G is the gravity number (Yao, Hbibian, & O'Melia, 1971).

The attachment efficiency (α) is the proportion of collisions between particles and collector that results in attachment. It is generally calculated empirically with the equation:

$$\alpha = \frac{2d_c}{3(1-n)\eta_0 L} ln\left(\frac{C}{C_0}\right) \quad (2.9)$$

Where d_c is the average diameter of the collector (m), n is the porosity (-), L is the length of the column (m), and C/C_0 is the normalized concentration of the injected particles (-) (Laumann, Vesna, Lowry, & Hofmann, 2013). Generally, the attachment efficiency is equal to 1 because favourable deposition conditions are considered.

According to Clean Bed Filtration Theory, deposited particles on porous medium grains do not affect further particles deposition on grains and there is a linear reversible attachment. Therefore, the removal of suspended particles is described by first-order kinetics, resulting in concentrations of suspended and retained particles that decay exponentially with distance (Hosseini & Tosco, 2013).

However, experimental evidence of deviation from this theory were reported for the presence of unfavourable deposition conditions, the presence of discontinuities and impurities on the grain surface, and particle deposition at grain-to-grain contacts. Indeed, the CFT has been developed for colloid transport under favourable deposition conditions. But, if deposition condition is unfavourable, it is possible to observe a deposition in the secondary minima, that is reversible. Moreover, the presence of discontinuities can provide preferential deposition sites, due to local variation of interaction potentials (Tosco, Bosch, Meckenstock, & Sethi, 2012).

2.4.3 Blocking, Ripening, Filtration Cake and Straining

Other phenomena could occur, that make DLVO and Clean bed Filtration theories not always fit to represent reality. They are shown in Figure 2.8 and they are shortly explained as follows:

- *Blocking* occurs when particle-particle interactions are repulsive, so particles tend to interact with porous medium when it is clean, then they reject other particles. Thus, after the attachment of the first particles to the porous media, they prevent further deposition (Tosco, Papini, Viggi, & Sethi, 2014). The blocking kinetics (Φ_i) can be described as:

  $$\Phi_i = 1 - \frac{s}{s_{max}} \quad (2.10)$$

  Where S is the particle concentration in the solid phase (-) and S_{max} is the maximum particle concentration retainable on the solid phase at given chemical conditions. It is related to the surface blockage operated by already deposited particles (Tosco & Sethi, 2010).
- *Ripening* occurs when particle-particle interactions are attractive, so particles tend to interact with porous medium when it is filled with other particles and therefore, there is an increase in attachment kinetics, until the porous medium is completely clogged. Thus, ripening affects porous medium properties, reducing permeability and porosity (Tosco, Papini, Viggi, & Sethi, 2014). The ripening kinetics (Φ_i) can be defined as:

  $$\Phi_i = 1 + A_{rip} S^{\beta_{rip}} \quad (2.11)$$

  Where S is the particle concentration in the solid phase (-), A_{rip} (-) and β_{rip} (-) are the ripening coefficients that define the interaction dynamics. For A_{rip} >0 and β_{rip} >0, the deposition rate increases with increasing concentration of attached particles (Tosco & Sethi, 2010).

- *Filtration cake* occurs when particles are larger than porous medium size, so they are not able to penetrate in the porous media. Thus, it is possible to observe the accumulation of an impermeable filter cake above the porous medium as soon as particles are retained. The permeability is decreased very quickly, until an impermeable layer above the porous medium is formed. If particles are small enough to enter the porous medium, they can be removed by straining in smaller pore space (McDowell-Boyer, Hunt, & Sitar, 1986).
- *Straining* is the trapping of colloid particles in the down-gradient pore throats that are too small to allow particle passage (Bradford, Yates, Bettahar, & Simunek, 2002). Therefore, it occurs when colloids are retained in pores that are smaller than a critical size. The magnitude of colloid retention by straining depends on both colloid and porous medium properties (Bradford, Simunek, Bettahar, Van Genuchten, & Yates, 2003). Indeed, the irregular shape of grains can strongly affect this phenomenon, because it can give rise to a wide pore size distribution, with small pores in which straining is more effective (Tufenkji, Miller, Ryan, Harvey, & Elimelech, 2004). The attachment mechanism (Φ_i) can be modelled as:

$$\Phi_i = \left(1 + \frac{x}{d_{50,s}}\right)^{-\beta_{str}} \quad (2.12)$$

Where x (m) is the length of the path of the particles in the porous media, β_{str} (-) is a fitting parameter which controls the shape of the particle spatial distribution, $d_{50,s}$ is the average diameter of the particles (Bianco, Tosco, & Sethi, 2018).

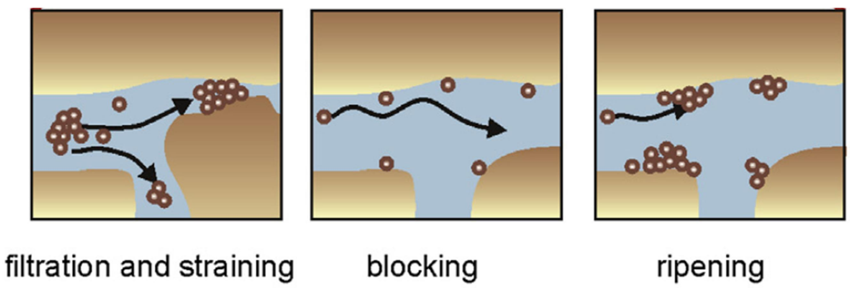

Figure 2.8: Representation of straining, blocking and ripening in a porous media. (Tosco, Papini, Viggi, & Sethi, 2014)

All the explained phenomena imply the deposition of particles within the pore space. This particle deposition reduces both permeability and pore space. Therefore, the decrease in pore space leads to a reduction in hydraulic conductivity and so to the progress of the clogging of the porous medium. The clogging is relevant especially when considering ripening, filtration cake and straining, while, for what concerns blocking, the reduction in porosity is generally negligible. Therefore, when clogging occurs, an increase in pressure is expected, if the flow rate is kept constant (McDowell-Boyer, Hunt, & Sitar, 1986). Filtration, straining, blocking and ripening, thus, could strongly influence experimental results and they must be kept into account. For this reason, different theoretical models have been presented (Tosco & Sethi, 2010).

Chapter 3

Materials and Methods

The aim of the project is to evaluate Al-OM mobility in porous media. For this reason, it is necessary to prepare different column experiments and determine the hydraulic conductivity during the course of the experiment. All parameters, such as the sand used, the solution concentration, the injected mass, and the packing, are kept constant in all the experiments and only the flow rate is changed.

The aluminium, the organic matter and the sand used during this research are presented in this chapter. Moreover, column experiment preparation and the procedures used are explained, to allow a reproducibility of those experiments. Some preliminary tests have been performed in order to better understand floc formation and the procedures followed are shown in the following paragraphs.

3.1 Chemicals and sand

The organic matter used in this research is a humic acid called HUMIN-P 775 and produced by the German biotech company HUMINTECH. It is a specially selected leonardite material which has been reacted with potassium compounds to neutralize the humic acids and to convert them to water-soluble potassium humates. It is soluble at low pH and the total organic carbon (TOC) is 42%, according to elemental chemical analysis performed by the University of Amsterdam.

The aluminium used is aluminium chloride hexahydrate ($AlCl_3$ * $6H_2O$), produced by Sigma Aldrich (CAS number 7784-13-6). It has a molecular weight of 241.43 g/mol and it is a crystal powder.

Sodium chloride (NaCl) is used as a background solution and as a conservative tracer to evaluate the pore volume (PV) of the columns used in the experiments. It is produced by Merck Millipore (CAS number 7647-14-5) and it has a molecular weight of 58.44 g/mol.

The sand used to fill the column is Dorsilit 8, a crystal quartz sand with a grain size distribution between 0.3-0.8 mm that has a high SiO_2 content (99.1%). Its density is 2.63 kg/dm^3.

All solutions are prepared with demineralized water. The background solution is prepared with a concentration of 1 mM of NaCl, while the tracer solution contains a concentration of 1 M NaCl. The Al-OM suspension is prepared with 1 g/l of OM and 10 g/l of aluminium chloride hexahydrate. The aluminium chloride hexahydrate, later on referred to as Al-chloride solution, is added to the OM solution to obtain a molar M/C molar ratio of 0.03. Values of pH, EC and DOM that have been measured of these solutions are presented in Table 3.1.

Table 3.1: Characteristics of the injected solution

Solution	pH	EC (µS/cm)	DOM concentration (mg/l)
Background solution (1mM NaCl)	6	170±4	-
Tracer (1M NaCl)	-	$70.49 \cdot 10^3 \pm 1$	-
Al-OM	4.7±0.1	426±6	25±4

3.2 Preliminary experiments

Three preliminary experiments have been performed to have a better knowledge about Al-OM interaction. The first experiment has the main objective of evaluating at which pH the OM is going to precipitate. The second one is carried out to determine the correct M/C ratio to obtain Al-OM flocs. Finally, the last experiment aims to evaluate how long it takes for flocs to settle.

3.2.1 OM precipitation at low pH

The aim of this experiment is to evaluate at which pH the OM would precipitate. Samples are filled with 60 ml of OM solution at 0.1 g/l. In each sample, an increasing amount of HCl 0.1 M is added and pH and EC are measured with Consort Multi-Parameter Analyser. As soon as the pH stopped to decrease significantly, the HCl concentration is increased to 2 M, in order to obtain a decrease in pH without the addition of an excessive amount of acid. The day after, the UV absorbance is measured, in order to evaluate in which samples the precipitation has occurred.

The same procedure has been repeated with a higher concentration of OM, equal to 1 g/l, in order to verify if the concentration used can affect the behaviour of the solution.

3.2.2 Al-OM flocculation

The objective of this experiment is to determine at which pH and molar M/C ratio aluminium and organic matter interact and precipitate. Samples are filled with 60 ml of OM solution with a concentration of 0.1 g/l. In each sample, a growing amount of Al-chloride solution at 1 g/l is added, until Al and OM start to flocculate. The absorbance has been measured the day after, in order to determine the samples in which flocculation has occurred.

A further analysis has been performed to better understand the correct M/C ratio to use for the suspensions that will be injected during column experiments. Thus, the procedure is the same used before, but the concentrations of OM and Al-chloride solution are respectively 1 g/l of OM and 10 g/l.

3.2.3 Sedimentation of Al-OM flocs

The aim of this test is to evaluate how long it takes for the flocs to settle, in order to better understand how to inject them. This is important since there is no stirring in the syringe pump that is used for the injection of the Al-OM suspension. For this reason, 1 l solution with 1 g/l OM has been prepared and the Al-chloride solution is added to obtain a M/C ratio of 0.03. The solution has not been subject to any stirring. A visual analysis has been performed, thus, a picture of the bottle is taken every two minutes, in order to see the evolution of the sedimentation.

3.3 Column experiment

The column used for the experiments consists of polyether ether ketone (PEEK), and is 22 cm high (H) and has a diameter of 5.4 cm (Φ). The total volume is 503.85 cm^3. It is placed in vertical position and the flow is from the bottom to the top. At the top and at the bottom of the column two circular filters are placed to prevent the spill of the sand from the column. Thus, the filter should be small enough to avoid sand release, and at the same time big enough to allow floc passage through it. For this reason, the filter dimension has been chosen to be 323.90 µm. The solutions and suspension are pumped through the column with a syringe pump, model 260D, ISCO, Beun De Ronde. Six pressure sensors Kema 30 ATEX 1561 are used, to measure pressure and to calculate hydraulic conductivity along the column continuously. Two pressure sensors, able to measure till 60 bar, are connected one to the inlet of the column (P_{in}) and the second to the outlet (P_{out}). Then a pressure sensor of 40 bar (DP1) measures the pressure drop between the inlet and the first 5 cm of sand. Another pressure sensor of 16 bar (DP2) measures the pressure drop between 5 cm and 11 cm. The next pressure sensor of 3 bar (DP3) measures the pressure drop between 11 cm and 17 cm and finally the last pressure sensor of 3 bar (DP4) measures the pressure drop between 17 cm and the outlet. The set-up configuration is showed in Figure 3.1.

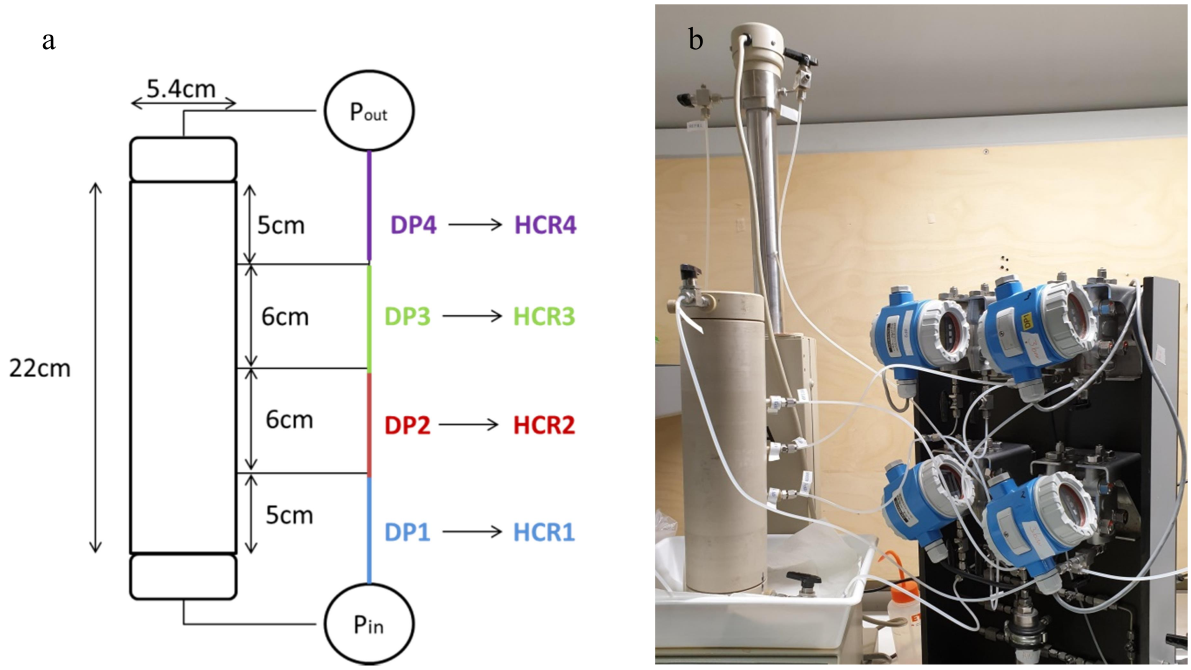

Figure 3.1: Experiment set-up: a diagram with the position of the pressure sensors and the sections along which the variation of the pressure is measured (DP), thus, according to the variation of the pressure, the hydraulic conductivity reduction (HCR) can be derived (a); a picture of the column with the pressure sensors (b).

In Figure 3.1 a, a schematic representation of the column with the position of the different pressure sensors and column dimensions are presented. In Figure 3.1 b, instead, a picture of the column and pressure sensors is presented.

3.4 Procedure of the experiments

The following steps are carried out for each experiment:

- Column packing
- Tracer test (1 M NaCl)
- Injection of the Al-OM floc suspension (1 g/l OM input concentration) at different flow rates
- Settling time (1 hour resting)
- Flushing of the column with background solution (1 mM NaCl)
- Removing sand from the column to visually evaluate floc distribution along the column

3.4.1 Column preparation

The column is dry-packed with Dorsilit nr. 8, with an increase in the sand level of 1 cm at a time. Every time that the sand is loaded in the system, a mechanically hand packing is performed, shaking the column with a hammer and then pressing the sand with a pestle. This procedure is repeated 22 times until the column is filled with sand. The column is weighted before and after the packing to evaluate the amount of sand put into it. The mass of sand is kept constant at a value of 846.64 g.

The column is closed and connected to the tubing which have been cleaned and dried. The column is then connected to a vacuum pump for a few minutes, to eliminate air from the system, and afterwards it is flushed with CO_2. Flushing the soil column with carbon dioxide prior to saturation should help to avoid air bubbles (Lewis & Sjöstrom, 2010). This procedure is repeated twice, before the injection of water at $8.3*10^{-8}$ m^3/s, to saturate the column. The flow is maintained from the bottom to the top of the column for the duration of the experiment, to ensure total saturation.

After the saturation of the column, all the lines are filled with water. Afterwards, the column is flushed at different flow rates to check that a complete saturation has been obtained and that the system works correctly.

3.4.2 Tracer Test

The tracer test is divided into a first injection of the background solution, as a preconditioning phase, then the tracer injection and finally the injection of the background solution, to flush the column from the tracer. The steps are summed up in Table 3.2.

Table 3.2: Tracer test steps

	Solution (M of NaCl)	Volume (ml)	Samples
Preconditioning	10^{-3}	200	20
Injection	1	600	60
Flushing	10^{-3}	400	40

The flow rate used is $6.67*10^{-7}$ m^3/s, so a Darcy velocity of $2.91*10^{-4}$ m/s, and a sample is collected at the outflow every 15 seconds to obtain 10 ml samples. The electrical conductivity of each sample is measured with Consort Multi-Parameter Analyser, in order to obtain a breakthrough curve. Starting from the breakthrough curve, it is possible to evaluate the pore volume, which is calculated as the moment at which it is obtained a value of EC equal to the half of the EC of the tracer (EC_0) (Fitts, 2013). The pore volume is the time required by a solution to flow through the column and it represents the volume of voids, so it is possible to evaluate porosity starting from its value. Indeed, porosity is defined as (Di Molfetta & Sethi, 2012):

$$n = \frac{V_v}{V_t} \quad (3.1)$$

Where V_v is the volume of voids and V_t is the total volume of the column.

In order to validate this calculation, the MNMs 2018 software has been used. MNMs is an acronym for Micro-and Nanoparticle transport, filtration and clogging Model – Suite. It is a software tool for the simulation of colloid transport in porous media, that provides also tools for tracer test interpretation (Tosco, Bianco, & Sethi, 2018). The model perfectly fit the data obtained during the tracer test, as shown in Figure 3.2.

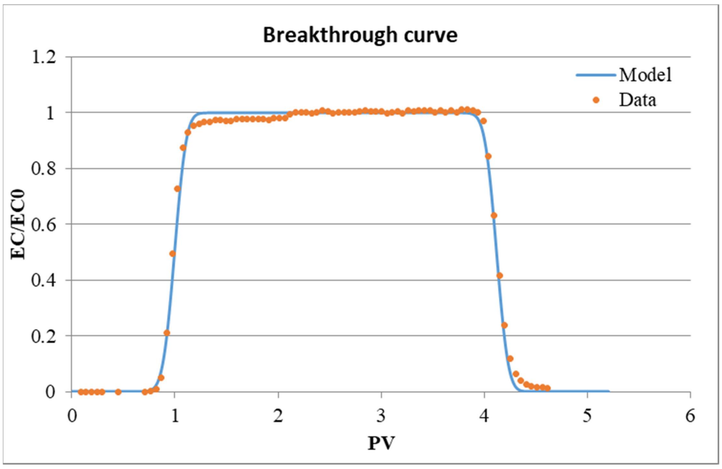

Figure 3.2: Breakthrough curve obtained by the tracer test injection: the orange dots represent the experimental data, while the blue line represents the model.

As it is possible to observe from Figure 3.2, at the beginning, the injection of the background solution presents an EC that is approximately zero, then there is an increase in EC due to the presence of the tracer and finally the background solution flushes the tracer away. The model is able to correctly fit the data and the values of porosity obtained by the calculation and by the model are comparable. All the values of porosity calculated and modelled and all the breakthrough curves are reported in Appendix A.

3.4.3 Floc injection

After the tracer test, the background solution is injected at the defined injection flow rate for that experiment. In this way, the initial hydraulic conductivity along the column can be measured. Afterwards, the Al-OM suspension is injected at the same flow rate. The suspension injected is always the same and two litres of suspension are injected at every test. The Al-chloride solution is added just before the injection and the Al-OM suspension is continuously stirred to avoid floc sedimentation. Pressure is continuously measured during the injection to calculate the variation in hydraulic conductivity along the column. Moreover, the total outflow is collected and weighted and 10 ml samples are collected every PV, to determine when flocs reach the end of the column. EC, pH and the UV absorbance at 254 nm of these samples are measured in order to evaluate the characteristic of the outflow and the amount of DOM present in the outflow.

Different tests have been performed to see how the system is affected by the injection rate. Every experiment is repeated twice, in order to show the reproducibility of the results obtained. The experiments carried out are summed up in Table 3.3.

Table 3.3: Performed column experiments at the different flow rate tested

Experiment	Flow rate (m^3/s)	Darcy velocity v (m/s)	Injected volume (l)
1.1 and 1.2	$3.33*10^{-7}$	$1.46*10^{-4}$	2
2.1 and 2.2	$8.33*10^{-7}$	$3.64*10^{-4}$	2
3.1 and 3.2	$1.33*10^{-6}$	$5.82*10^{-4}$	2
4.1 and 4.2	$1.76*10^{-6}$	$7.71*10^{-4}$	2

The experiments at a flow rate of $3.33*10^{-7}$ m^3/s, which means a Darcy velocity of $1.46*10^{-4}$ m/s, have been performed four times in order to obtain reproducible results. Actually, even after four tests the results were not reproducible at this flow rate.

3.4.4 Flushing

After the injection, a resting period of one hour has been chosen to allow floc regrowth. Then, the background solution is injected at $8.3*10^{-8}$ m^3/s, to measure the variation in the hydraulic conductivity after the injection at natural groundwater flow conditions. The stop of the injection before the flushing can be considered analogous to the background flow, because the background flow is negligible, if compared to the injection flow rate. The flow rate used for flushing is 3.13 m/d, which is a very high value for a background flow if compared to typical conditions in The Netherlands. However, this flow rate is low enough to avoid a change in floc distribution along the column. Thus, floc distribution obtained during injection can be seen when the sand is pushed out of the column. Indeed, after the flushing, the column is dissected, in order to have the possibility to perform a visual analysis of floc distribution.

3.4.5 The outflow

The total outflow is collected and weighted and one 10 ml-sample every one PV is collected to evaluate its characteristics. EC, pH and UV absorbance at 254 nm are measured. The UV absorbance is measured with the Hach DR6000 spectrophotometer, in order to determine the OM concentration in the supernatant and thus the dissolved organic matter. The relationship between UV absorbance at 254 nm and DOM concentration is shown in Figure 3.3.

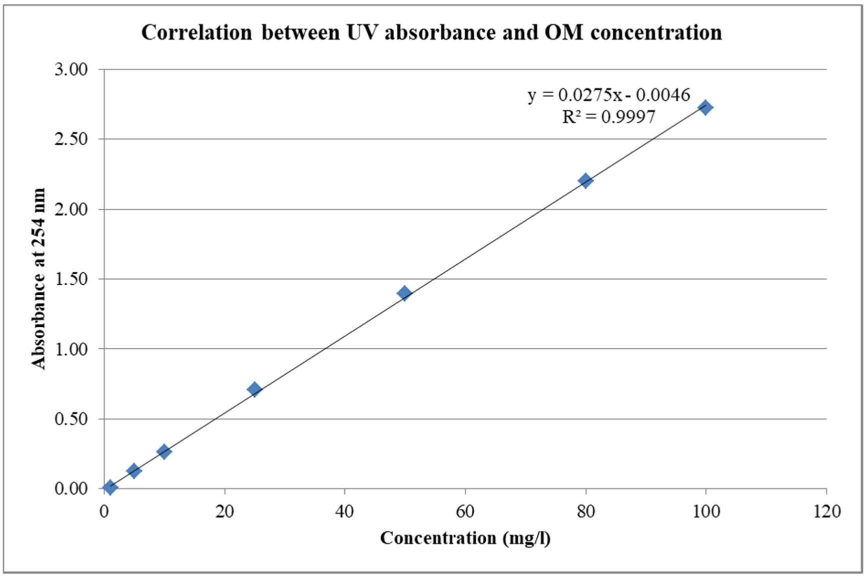

Figure 3.3: Correlation between DOM concentration and UV absorbance at 254 nm

This correlation curve has been obtained by preparation of a solution of 200 mg/l OM, which has then been diluted to different concentrations. The UV absorbance measurement at 254 nm has been performed for each concentration. The correlation depicted in Figure 3.3 is used to calculate the DOM concentration in the samples collected from the outflow and it is of particular interest for the samples collected during flushing. Indeed, these samples do not present flocs, thus, the DOM concentration is representative of the total organic carbon in the outflow.

A further analysis is the measurement of the total organic carbon (TOC) of the collected samples. Each sample that presents flocs is mixed and the TOC is measured with the Hach TOC cuvette procedure TOC LCK380/LCK381. First of all the sample is thoroughly shaken, then, it is added to a solution with oxidiser in a cuvette. After mixing with the oxidiser, the sample cuvette is closed with another cuvette which contains an indicator solution for CO_2. The sample is digested for 2 hours at 100°C to dissolve organic particles and oxidize the Carbon to CO_2. The formed CO_2 will flow through a membrane into the indicator solution in the upper cuvette. The colour change of the indicator solution is measured with the Hach DR6000 spectrophotometer. The method is checked for low range (LCK 380: 2-65 ppmC) and high range (LCK381: 65-735 ppm C) of organic carbon with a standard solution.

According to the values of TOC of the samples collected in the outflow, it is possible to estimate the mass of OM collected in the outflow, as presented in equation (3.2)

$$M_{out} = TOC_{out} * V_{inj} \quad (3.2)$$

Where TOC_{out} (mg/l) is the value of carbon of each sample measured in the analysis, V_{inj} (l) is defined as

$$V_{inj} = V_i - V_{i-1} \quad (3.3)$$

Therefore, V_{inj} is the difference between the total volume injected when the sample is collected (V_i) and the volume when the previous sample is collected (V_{i-1}). The collected sample is just 10 ml, but it is estimated that the TOC is almost constant during the injection before next sample.

Thus, the TOC measurement gives the possibility to estimate the mass of carbon present into the column, because of the mass conservation equation.

$$M_{inj} = M_{in} + M_{out} \quad (3.4)$$

Where M_{inj} (mg) is the mass that has been injected in the column, M_{in} is the mass that remains inside the column and M_{out} is the mass collected in the outflow. The mass of OM injected is known and it is confirmed by the TOC analysis of the initial concentration. The mass of carbon in the outflow is estimated as explained in formula (3.2), considering the TOC measured in the total sample collected in the outflow. Therefore it is possible to estimate the mass of OM present inside the column.

The values of TOC of the samples collected at the outflow, are also used in the model MNMs in order to obtain the breakthrough curve. The fitting of the data allows to estimate the transport mechanisms that occur in the porous media.

Chapter 4

Results and Discussion

In this section, the results of the preliminary experiments performed to better analyse the behaviour of the suspension and the results of the column experiments will be presented. Floc mobility and hydraulic conductivity reduction obtained in the different experiments will be discussed. In particular, three main aspects are investigated: the hydraulic conductivity reduction that can be achieved at different flow rates, the change in floc distribution according to the flow rate and finally how the flow rate affects the injection practice.

4.1 Preliminary experiments

In order to better understand floc behaviour in different condition, it is important to perform some preliminary analysis. In particular, the precipitation of the OM at low pH, the correct M/C ratio to obtain flocculation and the time required to flocs to settle have been investigated.

4.1.1 OM precipitation at low pH

The aim of the experiment is to evaluate the pH at which the OM start to precipitate. The 0.1 g/l OM solution is diluted with HCl, starting from a neutral pH, until a pH of 1.17 is reached. Then, the solution is allowed to stand for one day, in order to enable precipitation. It is visible starting from pH=1.97, as shown in the third sample in Figure 4.1.

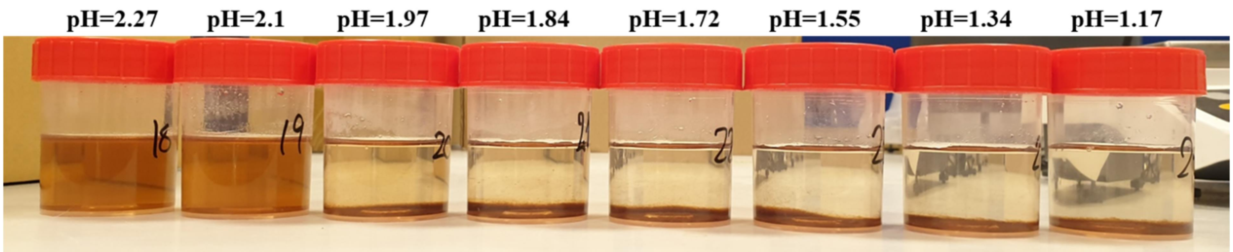

Figure 4.1: Precipitation of 0.1 g/l OM with decreasing pH

Figure 4.1 presents a comparison between the samples in which precipitation has occurred or not, with the value of the pH for each samples. It is possible to observe how the slight shift in the pH from 2.1 to 1.97 allows a different behaviour in the precipitation of the OM.

The experiment is repeated with a higher concentration of OM, 1 g/l, and the results are comparable, even though the precipitation starts at a pH equal to 2.39. The precipitation has been evaluated with the UV measurement at 254 nm, as presented in Figure 4.2.

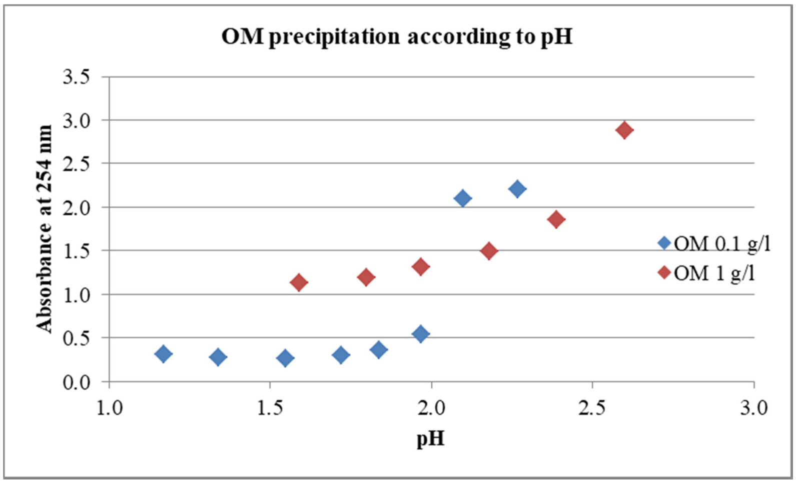

Figure 4.2: Precipitation of the OM solution at different concentration according to pH

As it is possible to observe from Figure 4.2, when the precipitation starts, the value of absorbance decreases sharply and remains almost constant. Therefore, the further decrease in the pH does not change the amount of OM that tends to precipitate. When the concentration is 1 g/l of OM, the precipitation occurs at a higher pH. This behaviour can be attributable to the increase in concentration, that allows an easier interaction between particles.

However, it is possible to conclude that the precipitation of the OM occurs at a pH around 2. The OM used for this experiments is a humic acid, which consists of that fraction of humic substances that are precipitated from aqueous solution when the pH is decreased below 2 (Pettit, 2014).

4.1.2 Al-OM flocculation

The objective of this experiment is to determine the molar M/C ratio that allows Al-OM flocculation. In the first tests, a concentration of OM of 0.1 g/l was applied, and the flocculation has been reached at pH 4.41, with a molar M/C ratio around 0.031.

In the second analysis with the OM concentration of 1 g/l, the flocculation occurs at a pH of 4.55 and a molar M/C ratio of 0.028, as it is possible to observe in Figure 4.3.

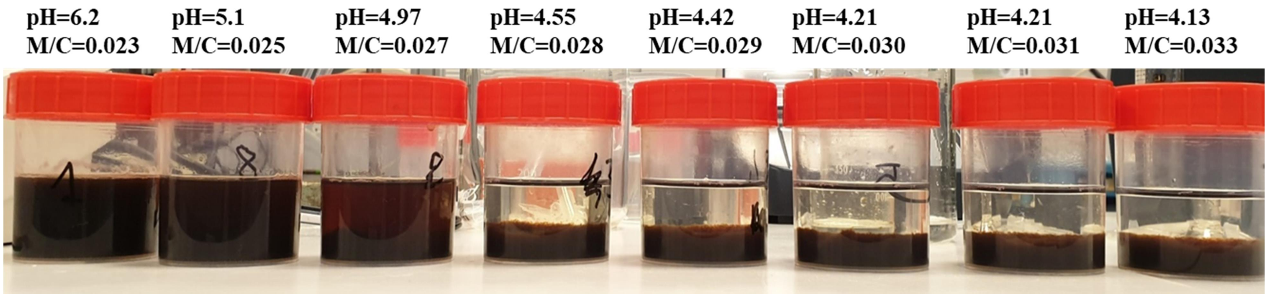

Figure 4.3: Al-OM floc formation and precipitation with increasing amount of aluminium.

Figure 4.3 shows the comparison between the samples in which flocculation has occurred and the ones in which it did not occur, with their respective values of pH and molar M/C ratio. The picture is taken the day after the experiment. The third sample on the left, which has a pH of 4.97 and a M/C ratio of 0.027, presents a beginning of flocculation, even though not complete as the next one.

The day after the experiment, samples are collected to perform the UV measurement at 254 nm, in order to determine the variation of OM present in the supernatant. The results are presented in Figure 4.4.

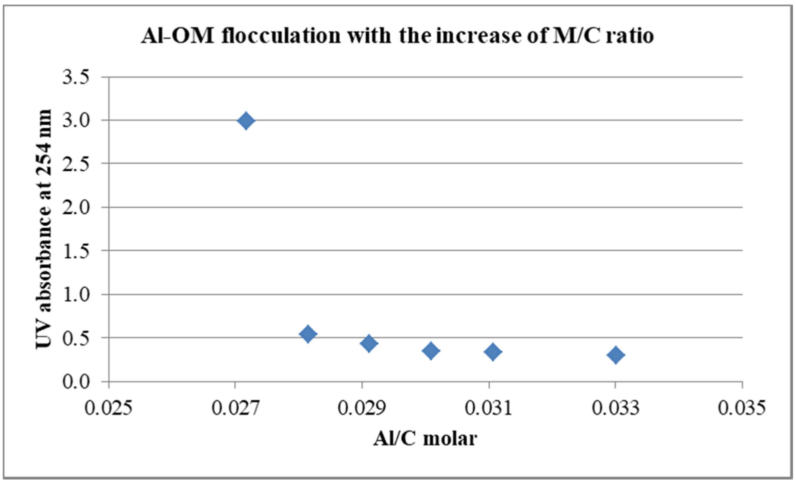

Figure 4.4: Al-OM flocculation and precipitation according to the Al/C ratio

Figure 4.4 presents the variation of the UV absorbance at different molar M/C ratio. The highest value of absorbance measured is obtained from the third sample shown in Figure 4.3. The absorbance of the first two samples cannot be measured, because it is higher than 3, thus, higher than the detection limit of the spectrophotometer. Therefore, only with a dilution of 100 μl of the sample and 900 μl of demineralized water, a value of 2.377 can be achieved. The dilution affects the value of pH, but does not affect the precipitation of Al-OM flocs, that does not occur. With the same dilution, the third sample presents an absorbance of 0.750. Thus, a partial flocculation has occurred, but it is still very limited, if compared to other samples. Even though samples are allowed to stand for two days, the flocculation of the third sample is not enhanced, so the M/C ratio is not enough to determine a complete flocculation.

According to this analysis, a molar M/C ratio of 0.03 has been chosen to prepare the solution injected in the column, in order to be sure to obtain flocculation, but avoiding an excess of aluminium. The addition of a larger amount of aluminium is not necessary because it would result in free aluminium in solution, if all OM bounds are saturated. The presence of free aluminium can decrease floc size and inhibit flocculation, because of charge repulsion between the free aluminium in solution and the aluminium bound to organic matter (Jansen, 2003). Moreover, the presence of aluminium that is not required for the process is undesired both from an economical point of view, because it is expensive, and for an environmental point of view, because it is a pollutant. Thus, it is necessary not to overcome the optimal M/C ratio.

4.1.3 Sedimentation of Al-OM flocs

The aim of the experiment is to determine the time required by flocs to settle. The 1 g/l OM solution is prepared and the Al-chloride solution is added, with a M/C ratio of 0.03. No stirring is applied to the solution. Every two minutes, a picture is taken, in order to see the trend of sedimentation. The first picture is taken 6 minutes after the addition of the Al-chloride solution, because sedimentation starts to be visible and, after 8 minutes, a significant precipitation has occurred, as shown in Figure 4.5.

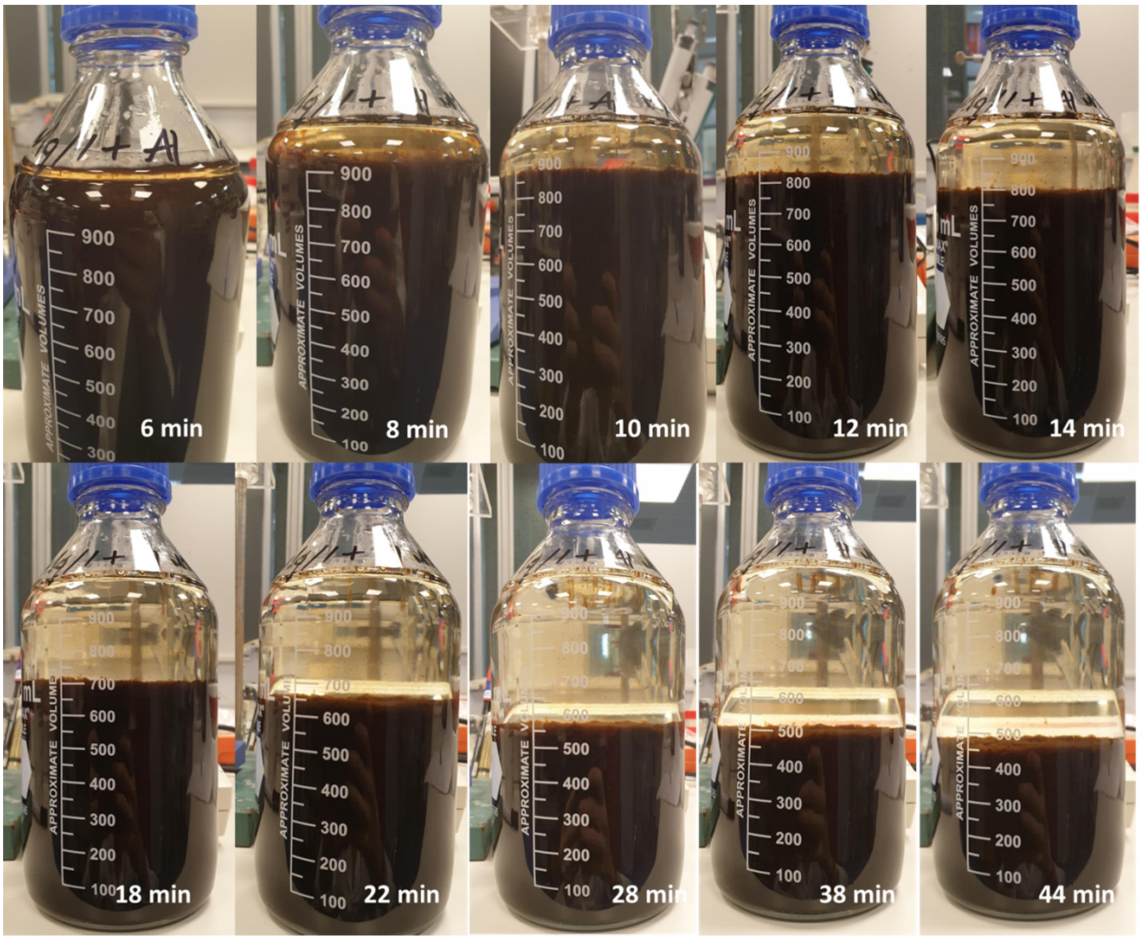

Figure 4.5: Precipitation of Al-OM flocs between 6 and 44 minutes without a previous stirring.

As possible to observe in Figure 4.5, a significant precipitation starts after 10 minutes and then it continues for almost 44 minutes, when the supernatant occupies half of the bottle. According to this analysis, the practical outcome for the transport tests is that it is important to avoid leaving the Al-OM suspension in the pump for more than 10 minutes. Otherwise, the suspension injected is no more formed by flocs but just by the supernatant, because in the pump there is no stirring.

4.2 Impact of flow rate on hydraulic conductivity reduction.

One of the main objectives of this research is to investigate which hydraulic conductivity reduction can be achieved by the injection of Al-OM flocs in porous media. Moreover, it is interesting to determine how this reduction is affected by the variation of the injection flow rate.

According to expectations, the highest HCR is obtained in the first part of the column, while it is less relevant in the rest of the column. Moreover, the HCR in the first part of the column decreases with the increase in the flow rate, as it is possible to observe from Figure 4.6. Here, only one result for each flow rate is presented, while the other results are presented in Appendix B.

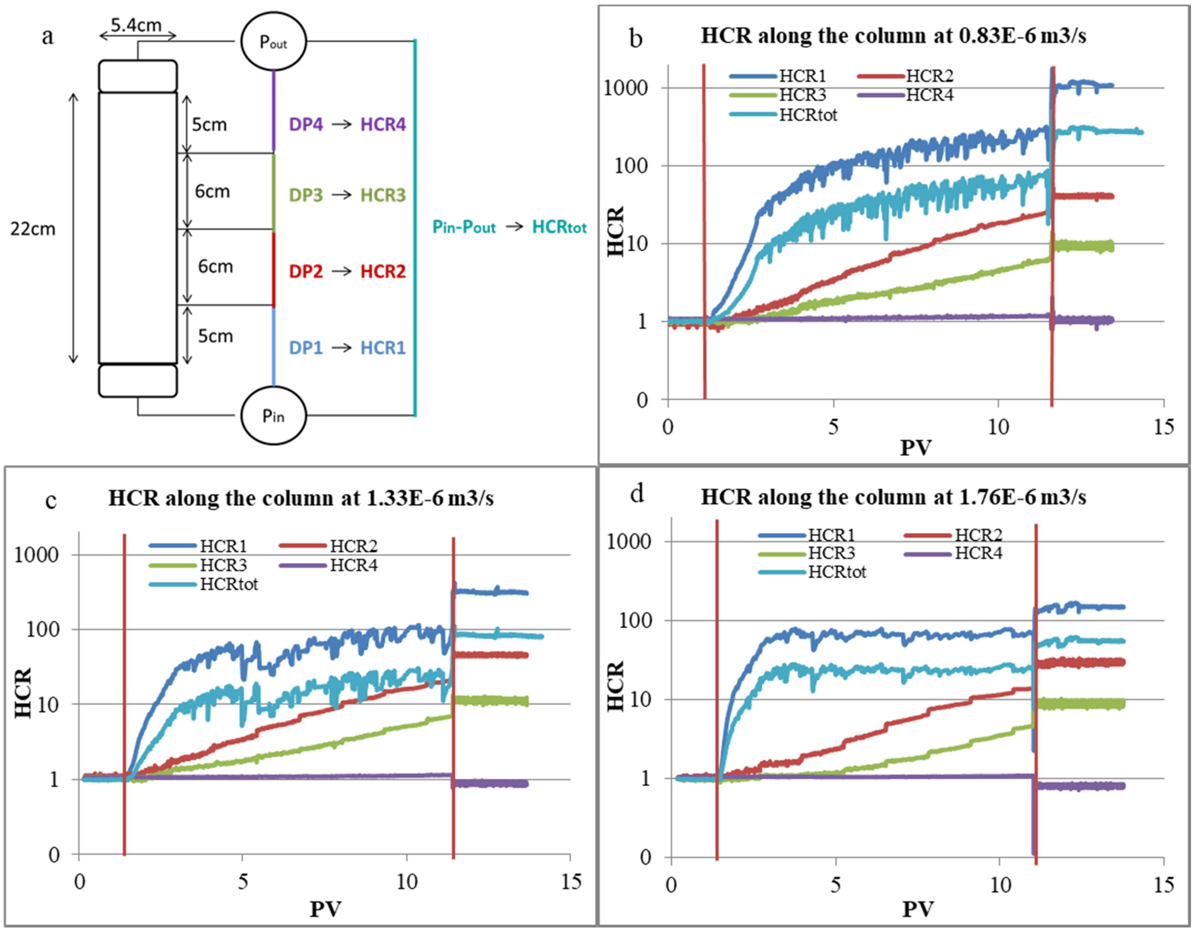

Figure 4.6: Hydraulic conductivity reduction during water and Al-OM floc injection at the different flow rates tested and during flushing at $8.33*10^{-8}$ m^3/s, in the different sections of the column.

Figure 4.6 presents, in Figure a, a schematic representation of the column, that allows to connect the position of the pressure sensors along the column and the corresponding hydraulic conductivity reduction that can be measured; in Figure b, c and d, the variation in HCR in the different sections of the column at the different flow rates considered, $0.83*10^{-6}$ m^3/s, $1.33*10^{-6}$ m^3/s and finally $1.76*10^{-6}$ m^3/s.

The first red vertical line, visible in Figure 4.6 b, c and d, marks the point where the injection starts, while the second red line marks the point where the flushing starts. For the first pore volume, the background solution is injected, in order to measure the initial hydraulic conductivity and so the reference point to calculate the HCR. Then, during the injection of 10 PVs of Al-OM solution, the graphs show an increase in HCR. Indeed, flocs enter in the system and start to clog the pores, thus they reduce the hydraulic conductivity. Finally, after stopping the injection for 1h, the column is flushed with background solution at $8.3*10^{-8}$ m^3/s.

Different conclusions can be drawn from the results presented in Figure 4.6. First of all it is important to observe that the highest HCR is in the first part of the column, where flocs are filtered by the porous medium. The biggest particles cannot be transported further and they remain connected to the first part of the column (Ryan & Elimelech, 1995). Therefore, most of the flocs remain near the inlet and the highest HCR is in the first part.

Moreover, the HCR in the first part of the column decreases with the increase in the flow rate. If the flow rate is increased, the shear rate is increased too. Therefore, Al-OM flocs are subject to higher shear rate and they decrease in their size (Jarvis, Jefferson, & Parsons, 2005). If particles are small, they are more mobile too and they can be transported further. As a consequence, less flocs remain trapped in the first part of the column and thus the HCR is lower, when the flow rate is higher.

A further evidence of the improvement of transport with the increase in the flow rate can be noticed by the different shape in the HCR curve in the first part of the column. All graphs present a strong increase in the HCR in the first 2 PVs, and then a smoother increase in the last 8 PVs. However, in the last part of the injection, with the increase in the flow rate, it is possible to obtain a certain stationary value, which is not obtained at the lowest flow rate. This behaviour can be explained by the fact that, at high flow rate, flocs can be transported further, after a first clogging of the porous medium. At low flow rate, instead, the HCR continues to increase, because flocs continue to be trapped in the first part of the column.

Another aspect that can be seen in the first part of the column is that data present strong fluctuations. Indeed, flocs enter in the system and start to clog the pores, but at the same time they are still influenced by the continuous injection that changes their structure and pushes them further in the column (Wang, Gao, Xu, Xu, & Xu, 2009). Therefore, the oscillations are probably due to a continuous formation and destruction of the flocs in the porous medium. They are more relevant in the first part of the column, where the biggest flocs remain. The second part of the column, instead, is less affected by this phenomenon of formation and destruction of flocs, because it is crossed by less and smaller flocs and the fluctuations are not so strong in the last part.

Another important element that can be deducted is that nothing relevant occurs in the last part of the column. In all the presented situations the HCR remains equal to one, thus there is not a variation in the hydraulic conductivity. This is probably due to the fact that only small flocs are able to reach the end of the column and they are not able anymore to aggregate and reduce the hydraulic conductivity.

Finally, the HCR during flushing is higher than the one measured at the end of the injection, for the first three sections of the column. This means that, when the injection is stopped, flocs are able to regrow, to aggregate and to create bigger structures that decrease pore space in the porous medium (Jarvis, Jefferson, & Parsons, 2005). This is an important conclusion because it shows that flocs are able to regrow not only in batch but also when injected into porous media, thus, the process efficiency can be increased by this mechanism.

In order to better compare all the obtained data about HCR, a sum up of all these results is presented in Figure 4.7

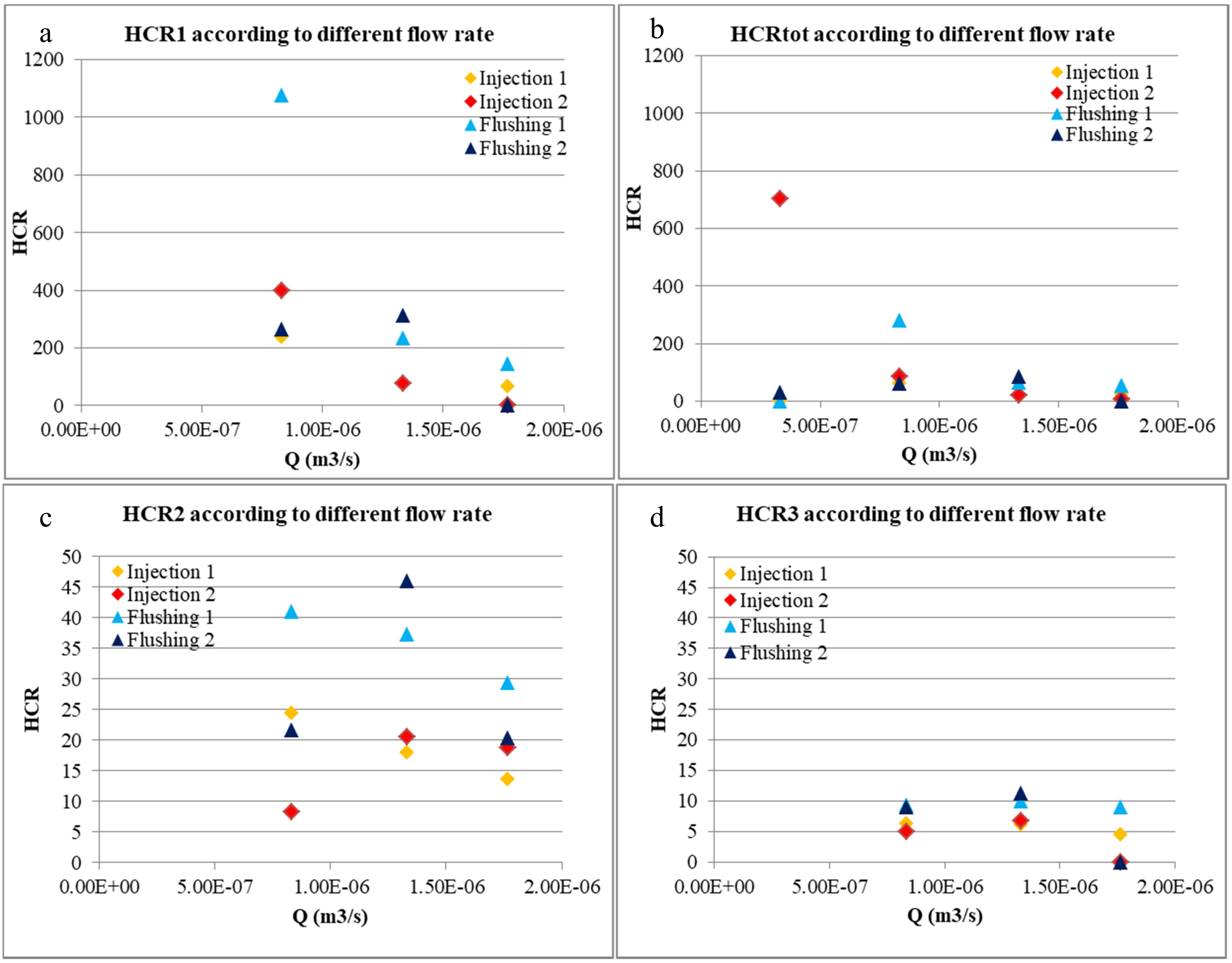

Figure 4.7: HCR calculated during the injections at $0.83*10^{-6}$, $1.33*10^{-6}$, $1.76*10^{-6}$ m^3/s and during flushing at $8.33*10^{-8}$ m^3/s in the different sections of the column

Figure 4.7 shows the effect of the variation of the flow rate on the HCR, before and after flushing, for all the performed experiments in the different sections of the column. HCR_1 represents the first 5 cm, HCR_2 the section between 5 and 11 cm, HCR_3 the section between 11 and 17 cm and HCR_{tot} represents the whole column and it is calculated starting from the pressure drop between P_{in} and P_{out}. In order to sum up the HCR during flushing in just one value, the mean of all values of HCR obtained during flushing is presented, for the considered flow rate and section of the column. On the other hand, to sum up the HCR during injection in one value, the mean of the last minute of injection is presented, which is the highest value that can be achieved.

According to Figure 4.7, it is possible to evaluate more in detail the variation of the HCR according to flow rate. At high flow rate, the difference between the values obtained from the two duplicates at the same flow rate, is smaller than at low flow rate. Indeed, most of the values of injection 1 and 2 are overlapped when considering a flow rate higher than $1.33*10^{-6}$ m^3/s. To better analyse this consideration, a summary of the values of HCR that are achieved during the first duplicate (X.1) and in the second duplicate (X.2) of the injection at the same flow rate is presented in Table 4.1

Table 4.1: Values of the total HCR and of the HCR in the first 5 cm of the column at different flow rate

	HCR_1		HCR_{tot}	
v (m/s)	**X.1**	**X.2**	**X.1**	**X.2**
$3.64*10^{-4}$	239	398	63	87
$5.82*10^{-4}$	79	76	22	20
$7.71*10^{-4}$	67	38	24	19

Table 4.1 presents the values of HCR in the first 5 cm of the column and the total HCR in both the experiments performed at the same flow rate. The variation in HCR between the two duplicates at the same flow rate is bigger for low flow rate. This can be explained by the fact that at low flow rate flocs are bigger and their interaction and clogging can vary significantly in the first part of the column.

Another important aspect that can be derived from Figure 4.7 is that the HCR in the second and third part of the column is not seriously affected by the change of the flow rate. The values of HCR obtained during flushing are all around 40 times in the second part of the column and around 10 times in the third part of the column, with slight differences. This behaviour is different from what it was expected. According to the previous analysis, if the flow rate is high, flocs are small and more mobile. Therefore, it is expected to obtain more flocs and thus a higher HCR in the second and third part of the column with the increase in the flow rate. However, according to the presented results, there is not an increase in the HCR in the second or third part of the column with the increase in the flow rate. Nevertheless, the HCR in the first part of the column decreases with the increase in the flow rate and the amount of flocs, that can be observed in the outflow, increases with the increase in the flow rate. A possible explanation can be connected to the deposition time. On the one hand, at low flow rate, in the second and third part of the column, there is a small mass of flocs because they are less mobile, but the deposition time is high, because of the low flow rate. Thus, flocs are able to interact and reduce the hydraulic conductivity during the injection. On the other hand, at high flow rate, the mass of flocs in the second and third part of the column is high because flocs are more mobile, but the deposition time is low. Therefore, with high flow rate, the deposition time is not enough for flocs to interact and to reduce the hydraulic conductivity, as much as it can be expected by the presence of more mass. Moreover, it is possible that, at high flow rate, floc structure changes so much that their ability to regrow and reduce the permeability has been decreased. Nonetheless, it is necessary to collect more data to have a better knowledge of this behaviour.

In Figure 4.7, it is also possible to better analyse floc regrowth. During flushing it is not always possible to observe an increase in HCR, especially in the first part of the column, Figure 4.7 a, and in the total value, Figure 4.7 b. Instead, in the second part of the column, Figure 4.7 c and in the third one, Figure 4.7 d, the increase in HCR after flushing is always visible. This increase in HCR during flushing is connected to floc regrowth in the porous media, as previously explained. This phenomenon can be strongly affected by the shear rate at which flocs have been subject (Yu, Gregory, & Campos, 2010). Therefore, in the first part of the column, where there are more flocs and higher pressures, data are much more disturbed and it is possible that flocs have been destroyed to such a small size that they are not able to regrow anymore. For example, in the second experiment performed at $0.83*10^{-6}$ m^3/s, the pressure that has been achieved is higher than the previous experiment at the same flow rate, thus, it is possible that flocs are no more able to regrow to a significant dimension. In addition, it is generally possible to observe a higher regrowth when the flow rate is low, because flocs have been subject to a lower shear rate and thus are able to regrow to a bigger size (Jarvis, Jefferson, & Parsons, 2005).

Another necessary consideration is about the experiments in which the flow rate of $0.33*10^{-6}$ m^3/s is chosen. They are presented only in Figure 4.7 b, where the HCR is calculated as the difference between the pressure at the inlet and the one at the outlet, because, during these experiments, only the pressure at the inlet and at the outlet was measured. For what concerns the second injection at $0.33*10^{-6}$ m^3/s, the HCR presented is the mean of the values measured during one minute in the sixth pore volume of injection. This is because, after this point, the HCR collapses to a low value, probably due to a fracture that occurred in the system. The pressure reached in this experiment is up to 25 bar, and then it collapsed to a low value, as shown in Appendix C. Therefore, there is the possibility that a fracture occurred in the system (Luna, et al., 2015). In the other column, instead, the highest pressure reached is 5 bar. The difference between those two experiments is thus so high that it is difficult to take into account those experiments in the analysis.

Finally, it is always important to look at the total HCR that is achieved. Most of the values that have been achieved after flushing are below 100 times of reduction. This can be considered a relevant result, but it is just a small scale reproduction of reality. In addition, the HCR obtained in the third part of the column is always below 10 times, which is a really low value, especially if it is taken into account that the distance from the injection point is just 17 cm. Therefore, it is still necessary to improve the technique to obtain better results.

For this reason, it is also interesting to analyse the comparison between the expectations presented in the first chapter and the real obtained results, as shown in Figure 4.8.

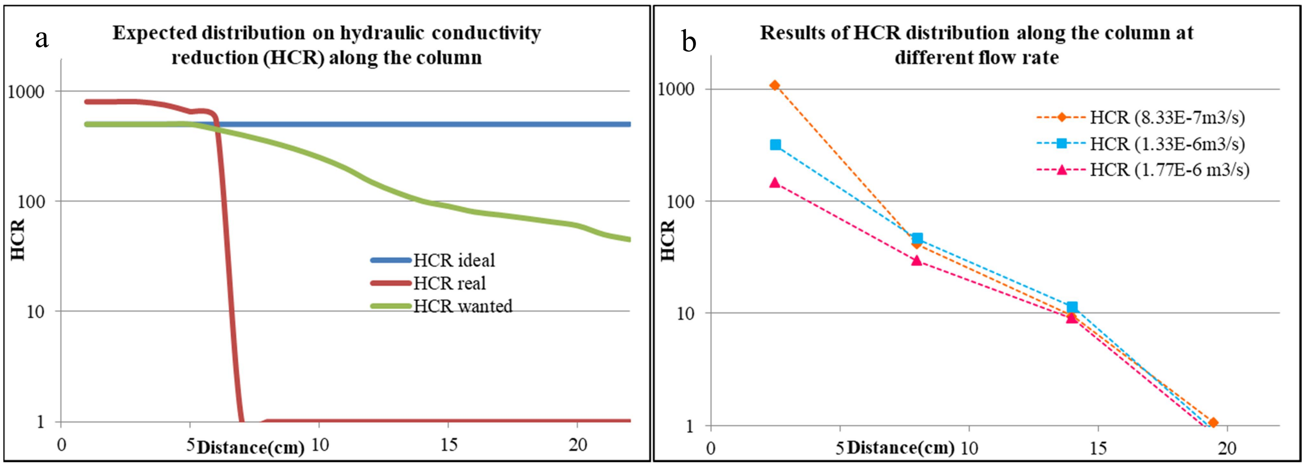

Figure 4.8: Comparison between the expected distribution of HCR along the column (a) and the values of HCR along the column obtained during the experiments at different flow rate (b)

Figure 4.8 presents, in Figure a, the expectation on the HCR distribution along the column, and, in Figure b, the distribution of HCR obtained by the experiments at the different flow rate. In particular, the values of HCR reported in Figure 4.8 b are the values of the first flushing presented in Figure 4.7.

As shown in Figure 4.8, the increase in the flow rate allows a decrease in the HCR in the first part of the column. Instead, the rest of the column is less sensitive to the change of the flow rate, as previously explained. However, it is possible to observe that the variation of HCR along the column is not as steep as what was presented in the expected real situation, because an HCR has been achieved both in the second and third part of the column. Nevertheless, the obtained results are still far from an homogeneous distribution of the HCR along the column and the HCR in the last 11 cm is not as relevant as desired, but there is still time for improvement. It is possible to change other parameters, such as the concentration or the injected mass and they could affect the transport in a more effective way.

4.2.2 Hydraulic conductivity variation

Till now, the evaluation was focused on the hydraulic conductivity reduction, however, it is calculated as the ratio between the hydraulic conductivity measured during water injection and the final hydraulic conductivity, as shown in equation 2.4. Therefore, it is interesting to analyse which value of hydraulic conductivity can be achieved due to floc injection. For this reason, Table 4.2 presents the values of hydraulic conductivity before, during and after the injection for both the experiments performed at different flow rate.

Table 4.2: Hydraulic conductivity in the first 5 cm of the column in all the experiments

Q (m^3/s)	**K_{1water} (m/s)**		**$K_{1injection}$ (m/s)**		**$K_{1flushing}$ (m/s)**	
	X.1	X.2	X.1	X.2	X.1	X.2
$0.83*10^{-6}$	$4.62*10^{-5}$	$4.73*10^{-5}$	$2.15*10^{-7}$	$1.38*10^{-7}$	$4.41*10^{-8}$	$1.86*10^{-7}$
$1.33*10^{-6}$	$4.03*10^{-5}$	$3.91*10^{-5}$	$5.13*10^{-7}$	$5.70*10^{-7}$	$1.76*10^{-7}$	$1.28*10^{-7}$
$1.76*10^{-6}$	$2.74*10^{-5}$	$1.57*10^{-5}$	$4.01*10^{-7}$	$4.40*10^{-7}$	$1.92*10^{-7}$	$4.18*10^{-7}$

The hydraulic conductivity presented in Table 4.2 is the mean of all values calculated during water injection, for K_{1water}, and the mean of all values calculated during flushing, for $K_{1flushing}$. The $K_{1injection}$, instead, considers the mean of the last minute of injection. The values of hydraulic conductivity presented are the ones measured in the first 5 cm of the column, because it is the most affected by reduction, as previously shown.

The initial hydraulic conductivity is almost the same in all the experiments and then it generally decreases of two orders of magnitude at the end of the injection, and during flushing it generally continues to slightly decrease. Thus, it is possible to obtain a relevant improvement of sandy material.

4.2.3 Kozeny-Carman calculation

The HCR can be achieved because the Al-OM flocs present in the porous media reduce the pore space. Therefore, it is interesting to evaluate the relationship between the porosity and the hydraulic conductivity reduction. In particular, the Kozeny-Carman equation is used to define the relationship between porosity and permeability, when the pore space is filled with particles (Costa, 2006).

If this calculation is applied to the performed experiments, the results of the injection at $8.33*10^{-7}$ m^3/s show that the porosity should decrease from 0.38 to 0.12, in order to obtain the total hydraulic conductivity reduction that has been achieved during the injection. This would imply a reduction of the porosity up to 67.8%. For the results of the injections at $1.33*10^{-6}$ m^3/s and $1.76*10^{-7}$ m^3/s the porosity should decrease to 0.17, with a reduction of 55.7%.

However, the volume of flocs that has been injected is just 2 ml. If the variation of pore volume due to the Al-OM floc injection is considered, as explained in the formula (2.6), the porosity that can be obtained after floc injection is almost 0.38 with a reduction around 1%. Therefore, it is unlikely to achieve a reduction of porosity up to 60% with such a small volume injected. Even if this calculation is repeated, taking into account that all the mass injected remains in the first 11 cm of the column, the final porosity that can be achieved is 0.19 with a reduction of 51%. However, this estimation considers that all the injected mass is trapped in the first 11 cm of the column and does not take into account that part of it is present in the rest of the column and in the outflow. The reduction of porosity up to 50% is an overestimation of the real reduction that can be achieved, but it is still lower than the value calculated with the Kozeny-Carman equation.

Therefore, the Kozeny- Carman equation is not able to model the phenomenon that occurs in the porous media with the injection of Al-OM flocs. The hydraulic conductivity reduction that can be achieved cannot be explained by the presence of flocs that fill the pore space, as predicted by the Kozeny-Carman model, because the mass that should have been injected, according to this model, is higher than the one injected. Instead, it is more likely that Al-OM flocs just clog the pore throat and thus prevent the flow through the pores (Ryan & Elimelech, 1995). In this way, a high hydraulic conductivity reduction can be achieved with the injection of just 2 g of Al-OM flocs.

Nevertheless, the HCR that can be achieved in the last 11 cm of the column is very low, around 10 times, as shown in Figure 4.7. As previously explained, this phenomenon can be established by the low deposition time and the small size of flocs. Indeed, in this part of the column, flocs are so small that require a long time for them to aggregate. However, a further possible reason of this low HCR is that the clogging mechanism is different. They could reduce the hydraulic conductivity no more with the clogging of the pore throat but with the filling of the pore space. Thus, the mass present in this part of the column is not enough to obtain a high HCR by filling the pore space.

4.3 Influence of flow rate on mass distribution

Another important aspect that must be analysed is the mass distribution of Al-OM flocs along the column, in order to evaluate their mobility. It can be derived both by the pictures of the sand after it has been pushed out of the column and by the analysis of the samples collected in the outflow.

The main conclusion that can be drawn is that with the increase in the flow rate, it is possible to obtain an increase in the transport of flocs and therefore the mass of flocs is more homogeneously distributed along the column.

4.3.1 Sand samples

As already explained, the increase in the flow rate implies an increase in floc mobility. On the one hand, flocs are small, because of the high shear rate at which they have been subject and, on the other hand, particle deposition decreases with increasing flow rate (Syngouna & Chrysikopoulos, 2011; Tosco, Bosch, Meckenstock, & Sethi, 2012).

A strong evidence of this behaviour is the comparison between the sand columns after the injection at different flow rate. Indeed, the dark colour, that represents the presence of flocs, is much more homogeneously distributed with the increase in the flow rate, as shown in Figure 4.9

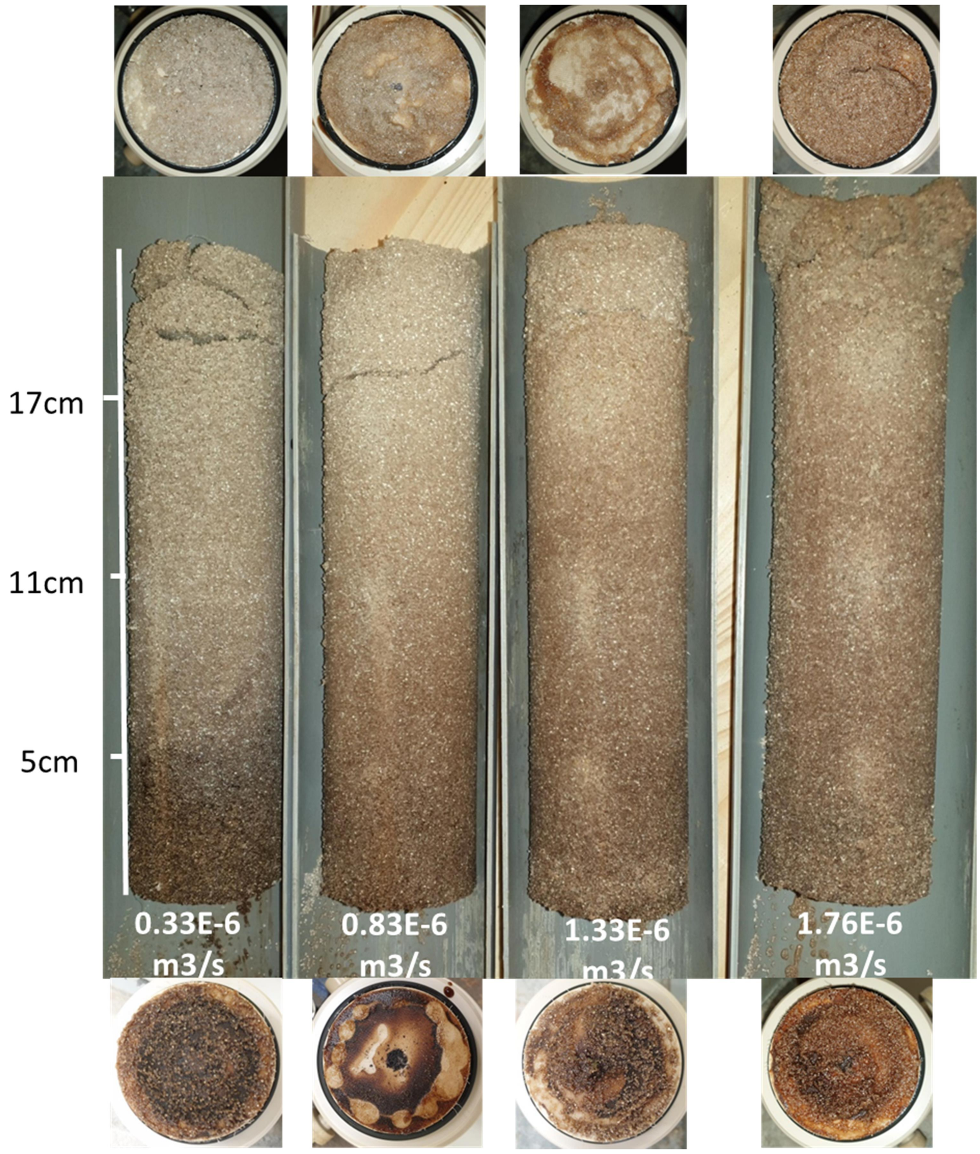

Figure 4.9: Picture of the sand pushed out of the column after Al-OM injection at different flow rate

Figure 4.9 presents the comparison between the sand extruded out of the column after the injection of Al-OM flocs at different flow rate and the pictures of the corresponding inlet and outlet. The column in which the lowest flow rate has been applied is shown on the left and then all the columns are sorted in ascending order of the applied flow rate.

As possible to observe in Figure 4.9, the dark colour, that represents the presence of flocs in the column, is differently distributed according to the flow rate, and, with the increase in the flow rate, a more homogeneous distribution is obtained. In the first column, at the lowest flow rate, the colour is very dark, but only in the first 5 cm. After this point, there is a marked change of colour that implies that flocs are not able to be transported further.

In the second column, instead, it is much more difficult to evaluate the point in which flocs are not present anymore, because the variation in the colour is smoother. In the first 5 cm of the column, the colour is still dark, but not as dark as the previous one. The reason for this observation is that flocs can be transported further and the injected mass is distributed along the first 11 cm of the column. The same behaviour is shown by the third column, where the variation in the colour is even smoother and a dark colour is visible up to 17 cm.

Finally, the last column presents the most homogeneous distribution of flocs along the column and also the last 5 cm are affected by the presence of Al-OM flocs. The first part of the column is still the darkest one, but the variation in the colour along the column is very smooth.

A further evidence of the improved homogenization of flocs distribution with the increase in the flow rate is given by pictures of the inlet and the outlet of the columns. It is possible to observe that the colour at the inlet shifts from a really dark colour to a lighter one. Instead, the colour at the outlet changes in the opposite way. It starts very light and in the last column is more brownish. This is confirmed also by the samples collected at the outflow, because it is possible to notice an increase in the mass of flocs in the outflow with the increase in the flow rate.

In conclusion, the presented results show that increasing the flow rate allows an increase in floc mobility and thus in their transport along the column (Tosco & Sethi, 2010). The mobility of Al-OM flocs along the porous media is strongly affected by the variation of the flow rate, even though the variation of the hydraulic conductivity reduction is not so relevant. This means that the mass of Al-OM flocs present in the porous media is not the only important parameter that allows a significant reduction of the permeability. Indeed, two other elements that affect this behaviour could be related to the deposition time needed by flocs to regrow and to the small size of flocs that are no more able to clog the pore throat.

4.3.2 Outflow

Another important element that allows to evaluate the transport of flocs along the column is the collection of samples in the outflow. The amount of flocs that is visible in the outflow is related to the injection flow rate. If the flow rate is high, it is possible to observe more mass outside the column, as it could be expected from previous observations.

Two elements have been considered: the DOM concentration in the supernatant and the TOC of the samples. The DOM decreases during the injection, because flocs start to settle in the outflow. This behaviour is visible at earlier PVs in the experiments at high flow rate, because flocs are able to reach the end of the column earlier at high flow rate than at low flow rate. The TOC increases at the beginning of the injection and then decreases during the flushing. Samples collected during flushing present a yellow colour, but no flocs at the bottom are found.

Both DOM and TOC have been used to determine the mass of the OM in the outflow, as presented in equation (3.2). The DOM is equivalent to TOC in the samples where there are no flocs.

A graph of the obtained results is presented in Figure 4.10.

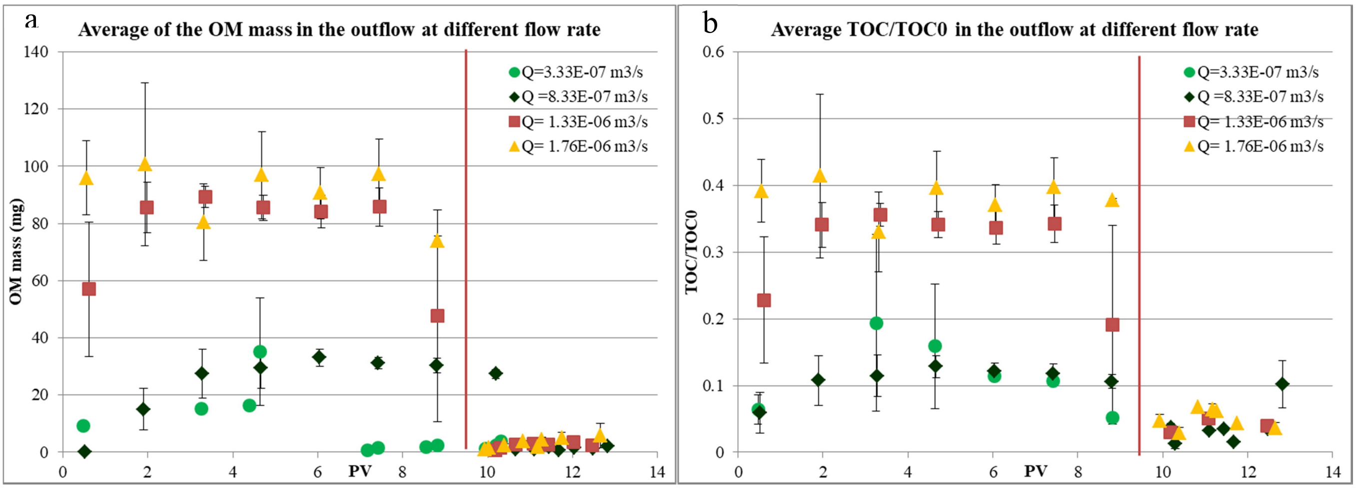

Figure 4.10: Mass of OM (a) and ratio between the TOC measured at the outflow and the TOC_0 of the injected suspension (b) measured in the outflow during the injection at different flow rate and during flushing at $8.33*10^{-8}m^3/s$

Figure 4.10 presents the mass of OM measured in the samples collected at the outflow, in Figure 4.10 a, and the ratio between the TOC of the sample collected at the outflow and the TOC of the injected suspension, TOC_0, Figure 4.10 b. The mass and the TOC considered are the average of the values obtained in the two duplicates at the same flow rate, with the corresponding standard deviation. The red vertical line marks the beginning of the flushing.

A first consideration that can be drawn is that the mass collected at the outflow during flushing is almost the same for all the experiments. The average of the total mass of OM collected during flushing is 15.4 mg ± 2.4. This value is so small that it can be concluded that the flushing is not able to mobilize flocs. Most of the mass that is collected during flushing is due to the presence of flocs in the lines before the beginning of the flushing. Therefore, if the flushing at $8.33*10^{-8}$ m^3/s is not able to transport flocs, the natural background flow, that is generally lower, will not be able to mobilize them. This conclusion is strongly relevant for the application of the technology in the field, because it means that once the barrier is built, it will not be moved.

The variation between the values obtained during the injection is very high, but it is still possible to observe the difference between the OM collected during the injection at low flow rate, the light and dark green signs, and the one collected during the injection at high flow rate, yellow and red signs. The mass collected at high flow rate is the double of the mass collected at low flow rate. Therefore, it is a further evidence that the transport of Al-OM flocs is increased with the increase in the flow rate (Zhuang, Tyner, & Perfect, 2009).

The mass that remains in the column, thus, is reduced with the increase in the flow rate. However, it decreases from 1.81 g, for the flow rate of $8.33*10^{-7}$ m^3/s, to 1.26 g for the highest flow rate. The average mass that remains in the column is 1.49 g. Therefore, almost the 60% of the injected mass is trapped in the porous media and it is able to reduce the total hydraulic conductivity up to 100 times.

Flocs are present in the outflow in most of the experiments that have been performed, with an increase in them with the increase in the flow rate, even if an effective permeability reduction in the last part of the column has never been reached. This could be explained by the fact that only the smallest flocs are able to reach the last part of the column, but they are so small that are not able to clog the pore throat. Moreover, at high flow rate when the mass of flocs is relevant also in the last part of the column, the deposition time is too low for them to regrow. Therefore, even if flocs are present in the last part of the column and in the outflow, they are not able to significantly reduce the hydraulic conductivity.

Increasing the flow rate, it is possible to obtain more flocs in the outflow and they are able to precipitate faster than flocs at a lower flow rate. When the concentration of flocs is small, it is more difficult for them to precipitate and it takes a longer time. For this reason, if the UV measurements are performed after more than 24 hours, it is possible to observe a general decrease in the obtained values, because flocs precipitate over time.

Finally, the electrical conductivity and the pH of all the samples have been measured, in order to evaluate the main characteristics of the solution in the outflow. The electrical conductivity presents an increasing trend that moves from the value of the background solution towards the value of the injected solution during the injection. While the samples collected during the flushing show the opposite trend that decreases towards the EC of the background solution.

The same behaviour is visible for what concern pH. Indeed, there is a decreasing trend of pH towards the value of the injected solution during the injection and then an increase up to the background solution value, during flushing.

4.3.3 Floc transport in porous media

According to all the reported results, it is possible to assume that two main transport processes occur in the porous media. On the one hand, in the first 5 cm of the column it is possible to observe a filtration of the particles, on the other hand, in the rest of the column, a certain attachment occurs.

In the first part of the column it is possible to observe a strong increase in pressure, that could be associated to the clogging of the porous media. The most probable reason of the clogging is the process of straining, according to which, the biggest particles remain trapped in the pores that are too small to allow their passage (Bradford, Yates, Bettahar, & Simunek, 2002). With the increase in the amount of particles retained in the first part of the column due to straining, the process of ripening is initiated. Therefore, the process of ripening increases the amount of particles that tend to attach to the porous media. For this reason, most of the mass stays in the first part of the column.

However, some small particles can still be transported further and in the second part of the column the attachment phenomenon is no more connected with filtration, because all the particles that are too big to cross the porous media have been trapped before (Bradford, Simunek, Bettahar, Van Genuchten, & Yates, 2003). In addition, the increase in the pressure is not as high as in the first part and it seems much more linear, as possible to observe in Figure 4.6. For this reason, it is likely that the attachment follows a first order kinetic, as in the clean bed filtration theory. Indeed, during flushing, it is not possible to observe flocs in the outflow, but still a yellow colour is present, which means that a part of the OM is coming out (Tosco, Bosch, Meckenstock, & Sethi, 2012).

In order to better understand the processes of attachment that occur into the column, the MNMs software is used to find the breakthrough curves able to fit the data of TOC collected in the outflow, as presented in Figure 4.11.

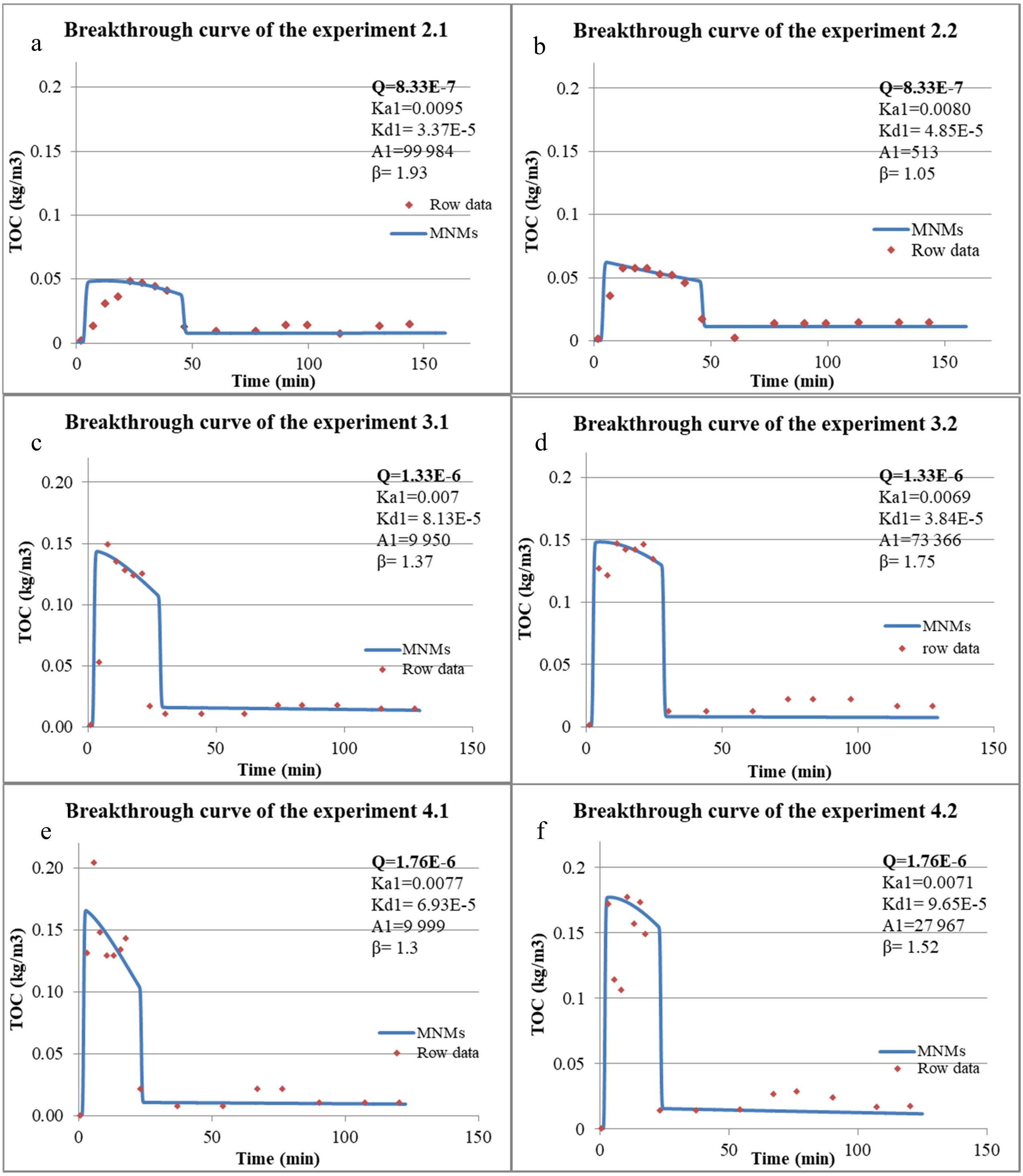

Figure 4.11: Breakthrough curves of the TOC measured in the samples collected at the outflow during the injection at different flow rate and during the flushing at $8.33*10^{-8}$ m^3/s

Figure 4.11 presents the data of TOC measured in the samples collected in the outflow and the fitting obtained from the model. In order to model particle transport in porous media, two attachment sites are considered: ripening, since it is the predominant process that increases the attachment, and linear attachment. A_1 and β are the ripening coefficients and they control the shape of the breakthrough curves. The decreasing trend of the breakthrough curves represents that the deposition rate increases with increasing concentration of attached particles (Tosco & Sethi, 2010). The attachment, k_{a1}, and detachment, k_{d1}, coefficients are comparable in all the experiments, even if the attachment is slightly higher in the experiments at low flow rate, Figure 4.11 a and b. This is consistent with the previous analysis, according to which the attachment decreases with the increase in the flow rate.

Therefore, according to Figure 4.11, even though there are a few data available and the model does not take into account the regrowth of flocs, the model is able to correctly fit the data. For this reason it is possible to conclude that the main transport processes are ripening and linear attachment.

4.4 Pressure behaviour according to flow rate

When an injection in the soil is considered, it is always important to take into account the pressure that is reached in the soil during the injection. For this reason, it is important to underline that, in the performed analysis, the pressure does not increase linearly with the flow rate.

It would be expected that increasing the flow rate, the pressure increases too, as it happens with water injection (Fitts, 2013). However, the behaviour is different, as presented in Figure 4.12.

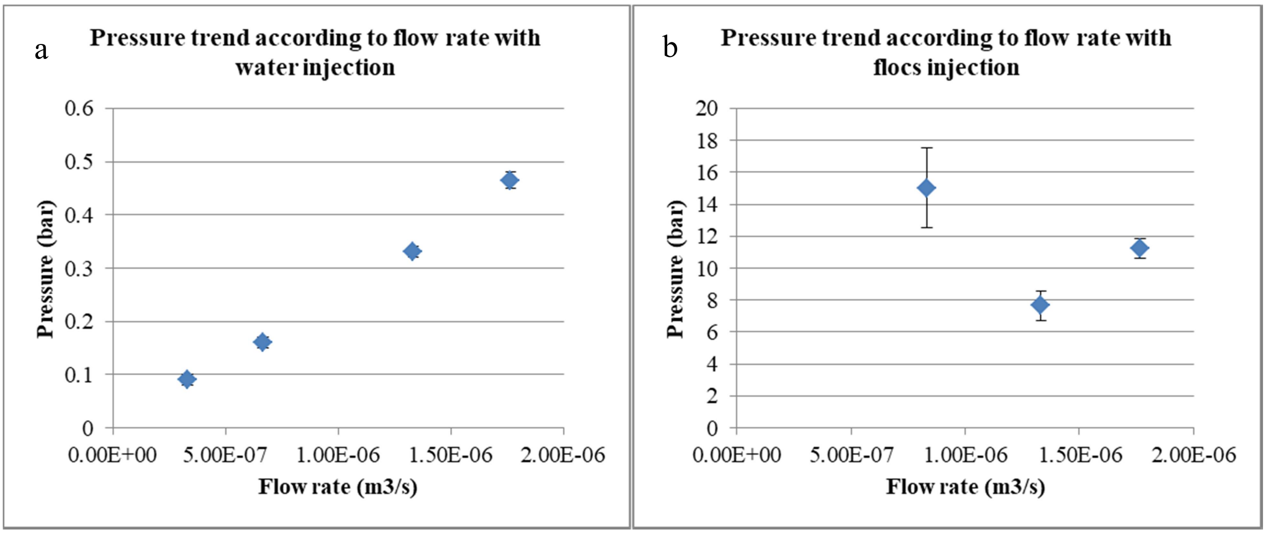

Figure 4.12: Comparison between the behaviour of the pressure according to the flow rate when it is injected water (a) and Al-OM flocs (b)

Figure 4.12 presents a comparison between the pressure behaviour during the injection of water and of Al-OM flocs. The pressure considered during floc injection is the highest reached at the end of the experiment. When water is injected in the column, pressure increases linearly according to the flow rate, as explained by the formula (2.3). Since the hydraulic conductivity is not affected by the presence of water, if the flow rate is increased, also an increase in pressure is expected, as presented in Figure 4.12 a.

When flocs are injected, instead, it is possible to observe a high pressure, up to 15 bar if the flow rate is low; while, if the flow rate is higher, the pressure is lower, around 10 bar. This behaviour can be explained by the change in hydraulic conductivity due to floc injection. Flocs clog the porous medium and thus decrease the hydraulic conductivity. Therefore, the relationship between the flow rate of injection and pressure is not linear anymore. It is possible to observe a decrease in the pressure with the increase in the flow rate. This unexpected behaviour can be explained by the different shear rate at which flocs are subject. If the flow rate is low, flocs are less mobile and remain trapped in the first part of the column, therefore the pressure is high (Zhuang, Tyner, & Perfect, 2009). Instead, if the flow rate is high, flocs are more mobile and the pressure is low. However, if the flow rate is very high, up to $1.77*10^{-6}$ m^3/s, flocs are small, but the pressure is still high because it is affected by the high flow rate.

Another interesting aspect, that can be drawn from Figure 4.12, is that the variation between the pressure values obtained in the duplicates at the same flow rate is higher at low flow rate than at high flow rate. The pressure measured at the flow rate of $0.33*10^{-6}$ m^3/s varies between 12 and 16 bar, while the pressure measured during the injection at $1.76*10^{-6}$ m^3/s varies between 10 and 11 bar. The values of pressure obtained during the injection at $3.33*10^{-7}$ m^3/s have not been considered, because they vary between 5 and 25 bar, so it is difficult to define a value. Therefore, this behaviour can be explained by floc size and transport. At low flow rate, flocs are bigger and can easily clog the first part of the column and thus the pressure increases. However, their behaviour is always different, according to their structure and their interaction with sand (Wang, Gao, Xu, Xu, & Xu, 2009). When the flow rate is high, instead, flocs are small and more mobile, and a lower amount is trapped in the column, thus the effect of floc interaction with sand is less relevant.

Finally, it is important to underline that the values presented in Figure 4.12 are the ones reached in the first part of the column and are the highest. The rest of the column, instead, is subject to a pressure that is no higher than 0.1 bar. For this reason, it is possible that a small fracture of the soil occurs in the first few centimetres of the injection, but then the pressure that can be achieved is not so high to be source of great concern.

4.5 Sources of errors

A final consideration that is important to take into account is about the factors that cause uncertainty of the results. A margin of error is inevitably present in the different performed experiments. This can be due to human error and to the precision of the instruments that are used during the analysis. Therefore, different elements, such as the porosity, the initial hydraulic conductivity and the suspension, can be subject to a certain variability even though they were supposed to be constant. Thus, these errors can lead to differences in the results obtained during the repetition of the experiments with the same boundary conditions.

4.5.1 Porosity

In order to keep the porosity constant, the column is always filled with the same mass of sand, which is 846.64 g. A fixed procedure to pack the column is followed in order to minimize the variation during this process. This procedure can be easily subject to errors, because the only parameter that can be measured is the mass of sand in the column, but it is not really possible to control the strength of the packing or the sand arrangement. Nevertheless, the mean of the values of porosity that have been derived from the tracer test is $0.38 \pm 1.5*10^{-3}$.

4.5.2 The initial hydraulic conductivity

Another aspect that should be constant at every experiment is the hydraulic conductivity that is measured during the injection of water. As explained in formula (2.3), it depends on the flow rate, the pressure, the packing of the column, the height and the cross sectional area of the column. Those two last parameters do not change, while the pressure, the flow rate and the packing can be affected by errors due to human error, to the precision of pressure sensors and of the pump that are used. However, those instruments can be considered very precise. The values of the hydraulic conductivity along the whole column are presented in Table 4.3

Table 4.3: Total hydraulic conductivity in the different experiments

Experiment	K_{tot} (m/s)
1.1	$1.22*10^{-4}$
1.2	$1.25*10^{-4}$
2.1	$5.15*10^{-5}$
2.2	$4.75*10^{-5}$
3.1	$4.73*10^{-5}$
3.2	$4.51*10^{-5}$
4.1	$4.20*10^{-5}$
4.2	$3.33*10^{-5}$
Mean	$6.42*10^{-5}$
Standard deviation	$3.46*10^{-5}$

As presented in Table 4.3, the highest variation is in the first two experiments that have been performed, therefore, it is possible that it is due to human error. Those two experiments were the first ones that have been performed, thus they can be less packed than the other ones. However, a slight variation in the initial hydraulic conductivity is always present, probably due to the packing of the sand in the column. Nevertheless, this variation is negligible if compared to the variation of hydraulic conductivity that is achieved during the experiments.

4.5.3 Al-OM floc suspension

Also the floc suspension can be a source of error even if it has been prepared in the same way, for example due to a weighing mistake or the accuracy of the balance. Therefore, an analysis of the total organic carbon present in the injected solution is performed, in order to better understand the characteristics of the injected suspension.

Table 4.4: Characteristics of the injected Al-OM suspension

Experiment	TOC (mg/l)	pH	EC (µS/cm)
1.1	396	4.89	424
1.2	416	4.77	420
2.1	425	4.63	430
2.2	393	4.67	420
3.1	398	4.47	428
3.2	394	4.73	439
4.1	380	4.81	420
4.2	392	4.56	421
Mean	399.3	4.68	426.1
STD	13.4	0.12	6.02

As it is possible to observe from Table 4.4, there is a small variation of the characteristics of the prepared suspension, but it can be neglected in the total analysis.

Moreover, also the background solution is subject to a variability because of human errors and the precision of the balance. However, the variation of this parameter is not so high to seriously affect the obtained results.

4.5.4 Values of UV measurements

The analysis of the samples collected in the outflow has been performed one day after the collection of the samples, in order to allow the sedimentation of flocs and an easy measurement of the supernatant. However, it has been observed that if samples stay still for a long time, and the UV measurement is repeated, the values obtained in this second measurement decreased. This can be explained by the fact that there are still small flocs in the supernatant that require a long time to settle. Thus, it is important to keep the time constant before measurement in order to ensure comparable results at all experiments.

4.5.5 Filter effect

Another important element that can influence the results is the presence of the filter in the column. In this case a filter is placed at the top and at the bottom of the column. The presence of a filter can affect the results, since it is possible that a filtration cake is formed before the filter due to floc filtration. In order to exclude this filter effect a preliminary experiment has been performed, in which the column is filled with gravel, so that the hydraulic conductivity reduction that can be observed during this experiment is only due to the presence of the filter. The procedure used for this experiment was similar to the ones for floc injection in sand. The injection rate was $1.33*10^{-6}$ m^3/s.

The results of this test show that the effect of the filter does not influence the overall results, as possible to notice in Figure 4.13.

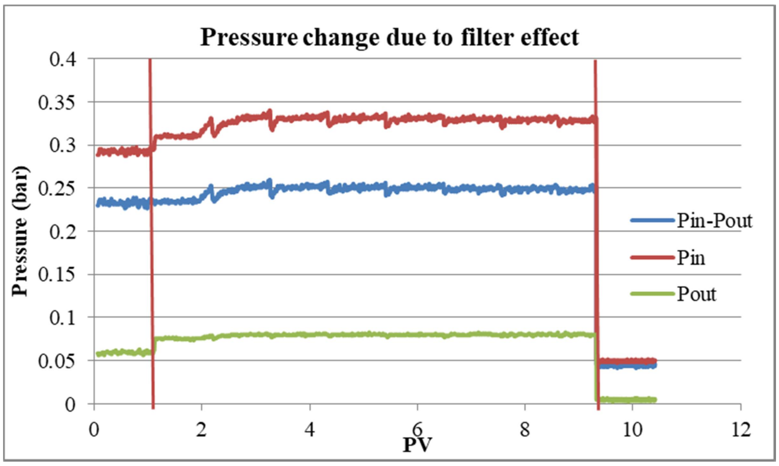

Figure 4.13: Values of pressure at the inlet and at the outlet of the column due to the presence of the filter, with the injection flow rate of $1.33*10^{-6}$ m^3/s.

It is possible to observe a slight increase in pressure in the first part of the column, especially for the pressure at the inlet, that evolves from 0.29 bar during the injection of water to 0.33 bar at the end of the last injection of Al-OM flocs. Based on this results it can be concluded that the filter contributes slightly to the overall increase in pressure and reduction in permeability at the first part of the column However, in any case, the effect of the filter is so small that it does not significantly influence the obtained results.

4.5.6 Experiment reproducibility

In conclusion, it is important to evaluate the reproducibility of the experiments. Each experiment is performed in duplicate to show that the obtained results are reproducible under the same conditions. However, it is always important to underline the fact that the discussed errors exist and can affect the reproducibility. In addition, the system used is a porous medium, so it is very hard to obtain the same results in this kind of configuration. Even though all parameters are kept constant, it is impossible to determine sand arrangement into the column. The highest uncertainty is about flocs, because they present a variable structure that cannot be totally controlled. They always flow and regrow in different ways in the porous medium. They can be destroyed and can form new structures, so it is impossible to obtain two identical results.

For most of the experiments that have been performed, it is possible to observe a satisfactory reproducibility. Indeed, in general, both pressure and hydraulic conductivity reduction are in the same order of magnitude and are comparable. The only exception is related to the experiments in which the flow rate of injection is $3.33*10^{-7}$ m^3/s, because they show a totally unpredictable behaviour. The maximum pressure reached in the different experiments varies between 1 and 25 bar. Moreover, when reaching such high values, the pressure then collapses to 1 or 2 bar. This behaviour can be explained by the formation of preferential pathways in the sand, following a re-arrangement of the grains due to the high pressure. For this reason, it is difficult to make a prevision about the results that can be obtained in these conditions. However, a common conclusion, that can be drawn from the experiment performed at $3.33*10^{-7}$ m^3/s, is that this flow rate is not high enough to allow flocs transport into porous media. Indeed, most of the mass remains trapped into the first 5 cm of the column.

4.6 Recommendations

The results that have been obtained in the performed experiments give different interesting information about floc mobility and the hydraulic conductivity reduction that can be achieved at different flow rate. However, data obtained are not enough for a statistical analysis nor to draw defined conclusions. Therefore, it is still necessary to further investigate the behaviour of Al-OM flocs, in order to have a better knowledge of the real processes that occur in the system.

A first suggestion is to measure the mass of flocs that is remained trapped in the different sections of the column, in order to make a correlation between the mass present in a certain section and the corresponding hydraulic conductivity reduction that can be achieved with that mass. In this way, it is possible to estimate the mass that is necessary to inject in order to obtain the desired hydraulic conductivity reduction.

The second suggestion is to repeat the presented experiments at least twice to confirm their reproducibility and to have a sufficient number of data to perform a statistical analysis. Moreover, a further investigation of the results that can be achieved with other flow rates can be useful to better understand the best flow rate in order to obtain the highest mobility and hydraulic conductivity reduction.

Another significant variation that can be analysed is the increase in the injected mass, in order to evaluate if it allows to obtain a higher radius of influence. With the increase in the injected mass, it is expected that more mass will be transported further and thus, that the hydraulic conductivity reduction in the last part of the column will be much more relevant. Therefore, it would be strongly remarkable, for field application, to understand if it is possible to increase the radius of influence just with the estimation of the injected mass.

On the other hand, it is also interesting to increase the OM concentration, in order to evaluate how does it affect the transport into a porous medium. The increase in the OM concentration can be a way to increase the injected mass but with a saving of time. However, it is necessary to evaluate the effect on the transport, because it is expected that the mobility of flocs will be reduced. The increase in concentration, actually, means the increase in the size of the Al-OM flocs and thus a reduction in their mobility. Therefore, the analysis can be focused on the correlation between the concentration of OM and the flow rate that allows the best mobility and hydraulic conductivity reduction.

An additional analysis can investigate the effect of the injection in different kind of sands and porosity. It is supposed that a reduction in the size of the sand and in the porosity would bring to a reduction in floc mobility and thus in the radius of influence. However, in order to apply this technology to reality, it is necessary to have the possibility to use it in different porous media and to make a prediction of what can occur in the different sand materials.

Finally, in order to better understand floc stability, it is important to study floc remobilization. In a field application, it could be necessary to inject new flocs after the first injection, to enhance the hydraulic conductivity reduction. However, it is not known if this injection could mobilize flocs present in the porous medium or not. Therefore, it could be estimated which is the flow rate that is able to remobilize flocs in a porous media.

Those are only a few suggestions that can help with the improvement of this technology. However, so many aspects still need to be investigated, in order to obtain a working technology that can be applied in the different fields of interest.

Chapter 5

Conclusions

The aim of this research is to investigate floc mobility in porous media. In particular, the effect of the flow rate on the transport of flocs in a porous medium and on the hydraulic conductivity reduction that can be achieved along the column has been investigated. Five main conclusions can be drawn according to the results that have been achieved:

- The transport of Al-OM flocs is strongly affected by the variation of the flow rate. When the flow rate is high, flocs are smaller and more mobile and they can be transported further.
- The main transport mechanisms that can be observed are straining and ripening in the first part of the column and a linear attachment in the rest of the column.
- The hydraulic conductivity reduction that can be achieved in the first part of the column decreases with the increase in the flow rate, while for the rest of the column the hydraulic conductivity reduction is not related to the flow rate of injection. Indeed, with the increase in the flow rate, a smaller amount of flocs remains trapped in the first part of the column and thus the reduction of hydraulic conductivity is lower. On the other hand, flocs present in the last part of the column do not have time enough to regrow and to reduce permeability. Moreover, they are too small to create a significant hydraulic conductivity reduction, even if the mass that is transported in the last part of the column is increased with the flow rate.
- A high hydraulic conductivity reduction has been achieved in the first 5 cm of injection for all the performed experiments, up to 300 times. Between 5 cm and 11 cm the hydraulic conductivity reduction is up to 40, while in the remaining 11 cm it is below 10 times. Therefore, the radius of influence is very small.
- The main mechanism that enables to achieve the high hydraulic conductivity reduction in the first part of the column is the clogging of the pore throats. This phenomenon allows to obtain a high hydraulic conductivity reduction with the injection of a minimum mass, if compared to the mass necessary to fill the pore space.

In summary, considering a future field application, the hydraulic conductivity reduction that has been achieved, within 11 cm from the injection point, is suitable for the building of a low permeable barrier, since, in general, it is possible to decrease the hydraulic conductivity of two orders of magnitude. However, some critical aspects exist in a field application. On the one hand, the distance at which a relevant hydraulic conductivity reduction can be achieved is really small, when considering the injection system and the length that is generally necessary to cover to create a barrier. On the other hand, the pressure that is generated during the injection is very high and, in the field, it could be the reason of the formation of fractures and preferential pathways that would make complex to create a continuous flow barrier, in the position where it was projected to be.

Therefore, further investigations should be focused on the increase in the injected mass, in order to very if it would allow to increase the radius of influence, and on the sand used during the experiments. It would be really important to perform different experiments in different kind of sands and porosities, in order to better understand the applicability of the technology to the different soils.

Appendix A

Here the results of porosity obtained from the calculation with the tracer test and with MNMs model are presented.

Experiment	Porosity	
	Tracer Test calculation	MNMs model
1.1	0.34	0.33
1.2	0.38	0.37
2.1	0.38	0.38
2.2	0.38	0.38
3.1	0.38	0.38
3.2	0.38	0.38
4.1	0.38	0.38
4.2	0.38	0.38

The breakthrough curves obtained from experimental data and from the model are presented for every experiment.

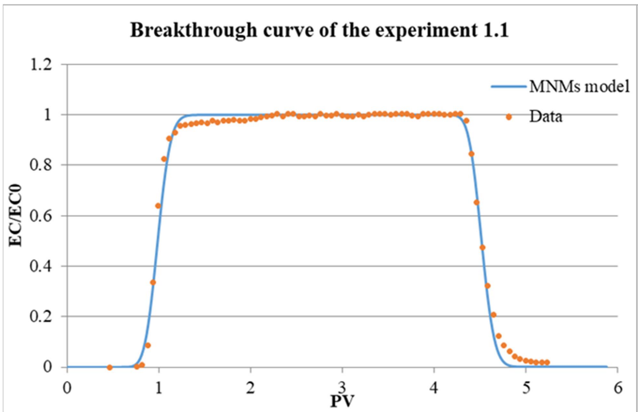

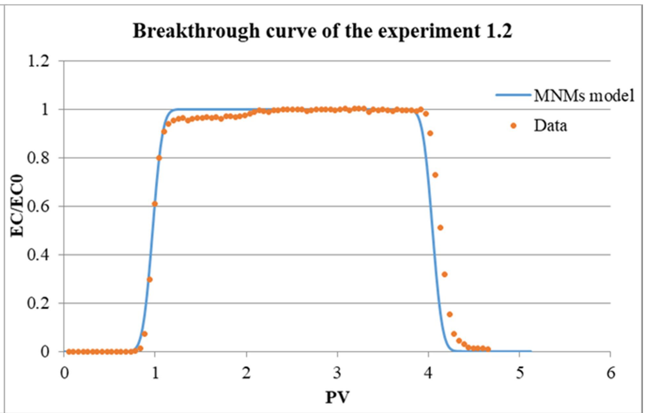

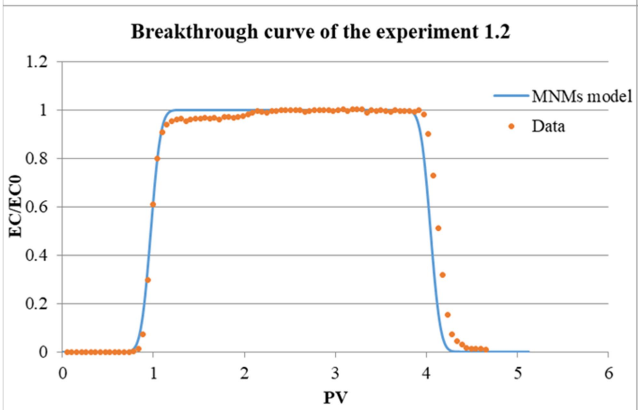

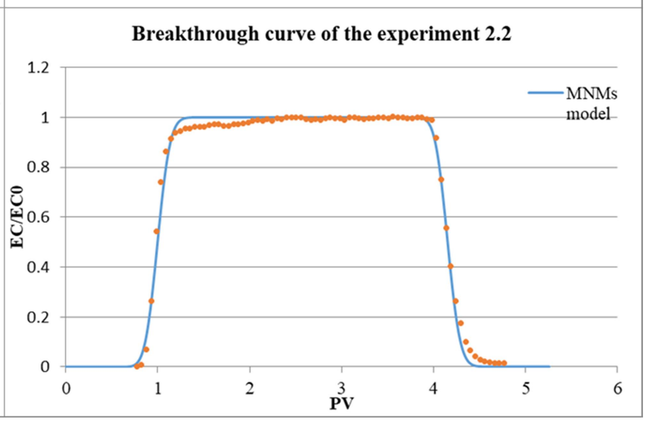

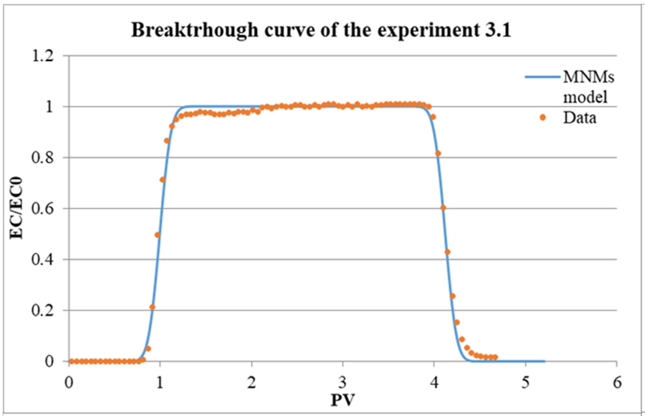
Breaktrhough curve of the experiment 3.1
EC/EC0
PV
MNMs model
Data

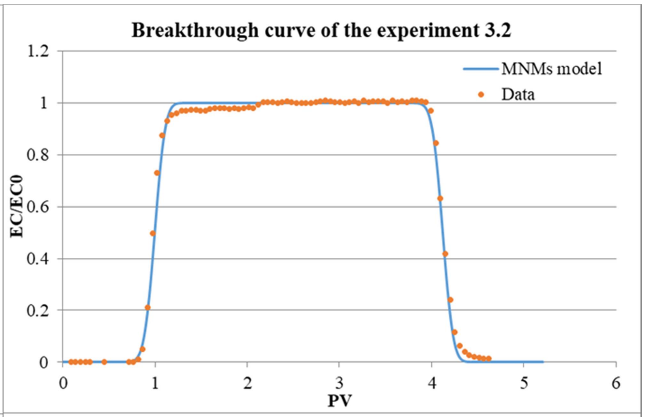
Breakthrough curve of the experiment 3.2
EC/EC0
PV
MNMs model
Data

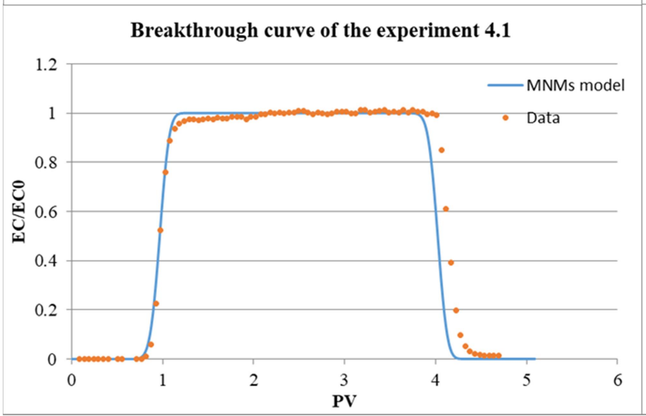
Breakthrough curve of the experiment 4.1
EC/EC0
PV
MNMs model
Data

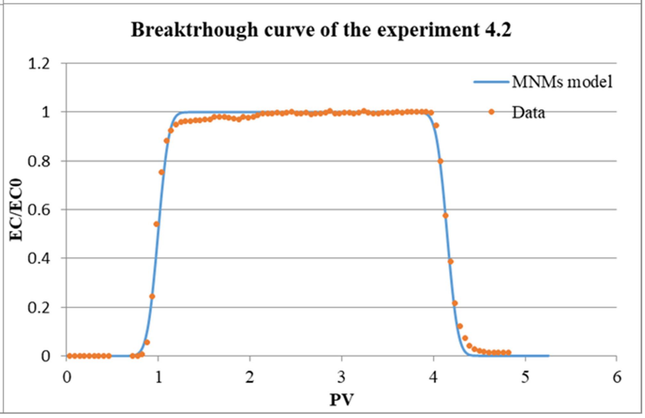
Breakthrough curve of the experiment 4.2
EC/EC0
PV
MNMs model
Data

Appendix B

Here the HCR obtained in the second trial of each experiment is presented.

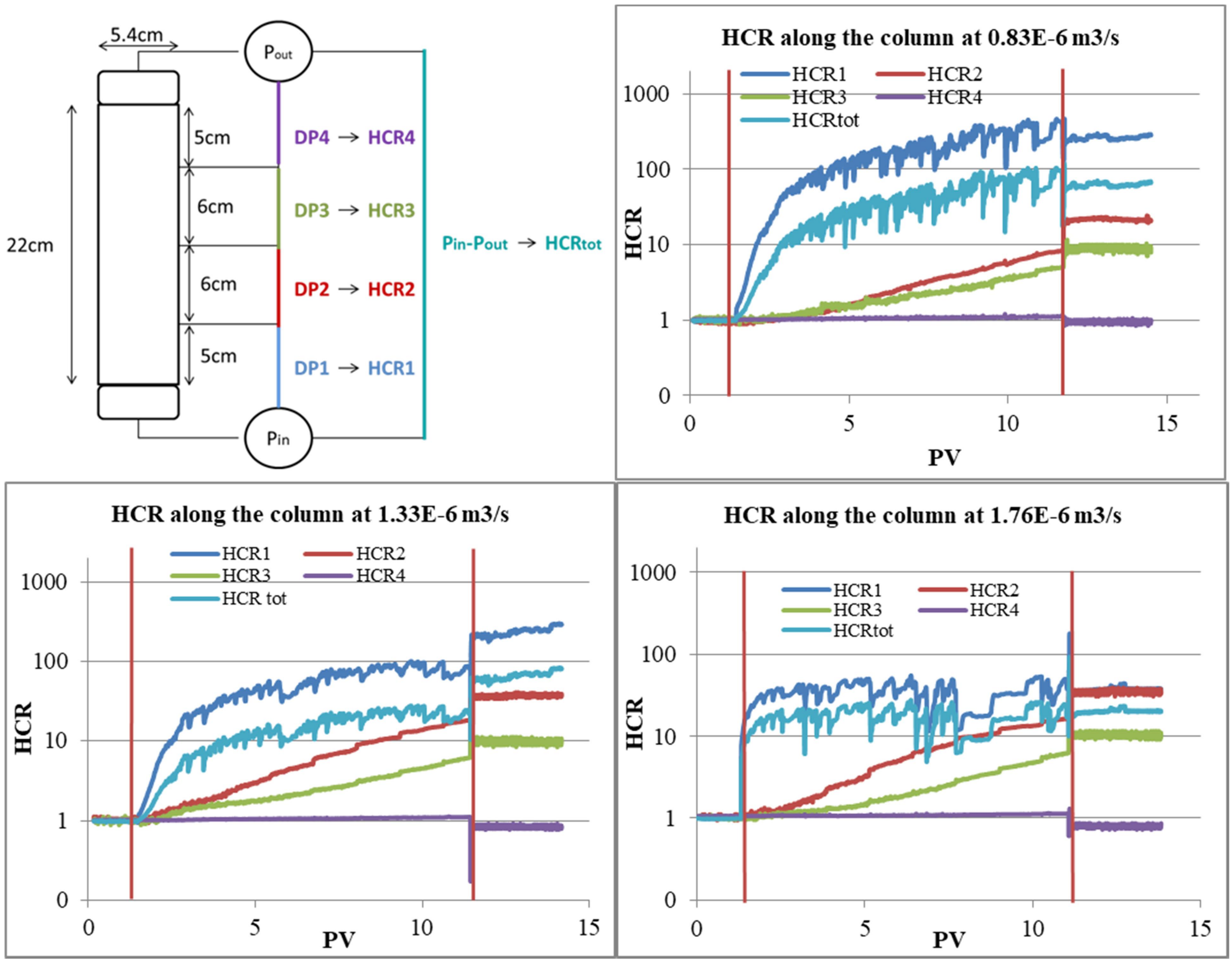

The pressure values obtained in the different experiments are also presented. During the injection of water, the pressure values in the first and in the last part of the column are higher than the values in the second and third part of the column. This can be explained by the presence of the localised pressure drop, due to the cross-section change from the size of the injection point, to the size of the column. Moreover the first and the last part of the column can be a little more packed than the rest of the column.

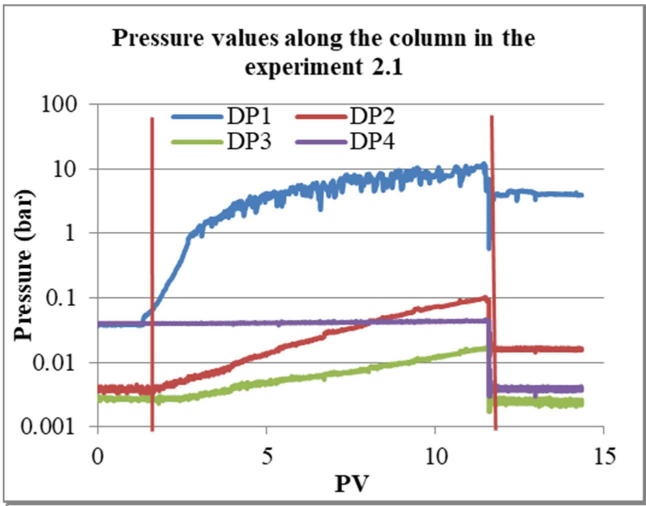

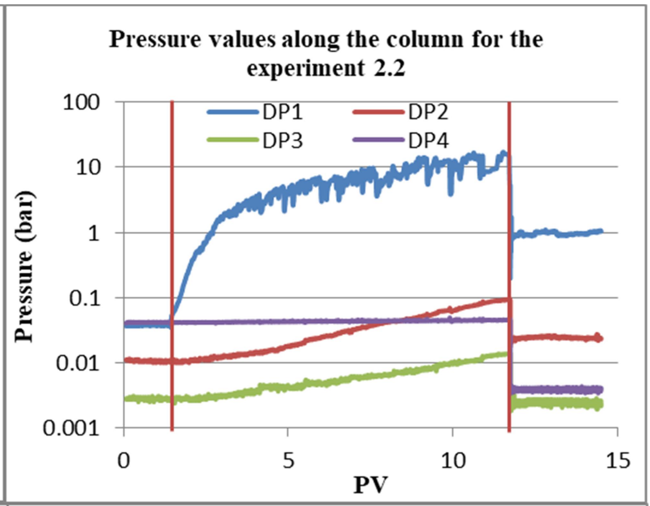

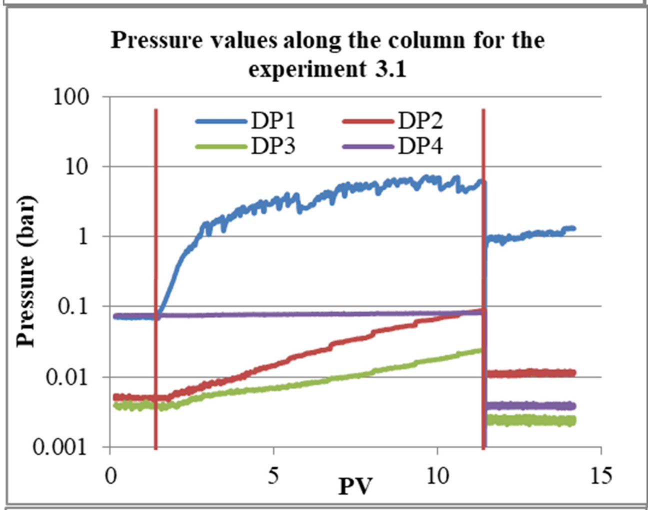

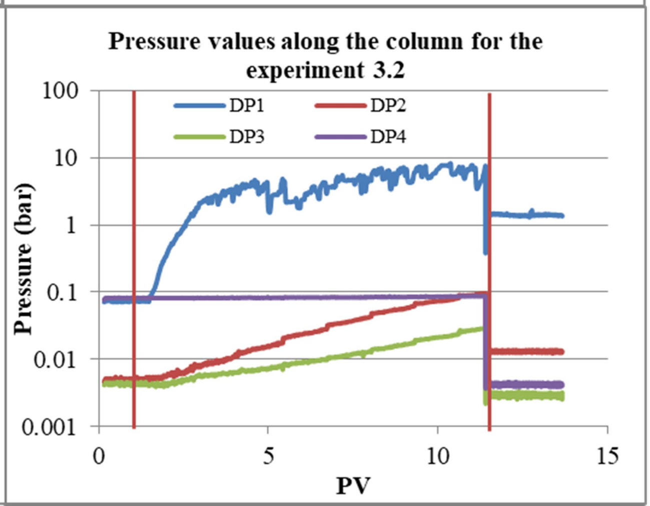

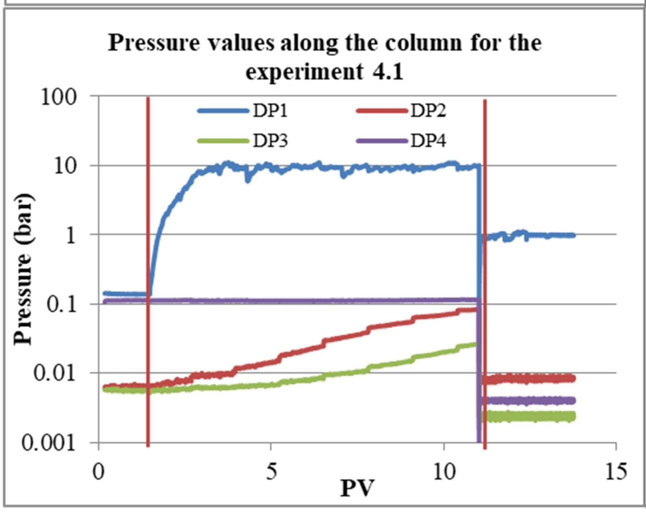

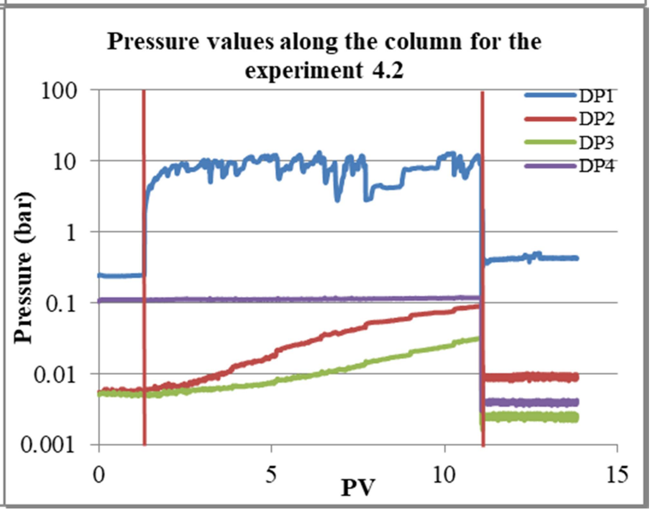

Appendix C

Here the results of the two experiments at $3.33*10^{-7}$ m^3/s are presented. They show that those experiments are not reproducible because both the values of pressure and HCR are totally different. Moreover the pressure trend of the experiment 1.2 explains the high probability that a fracture has occurred in the system.

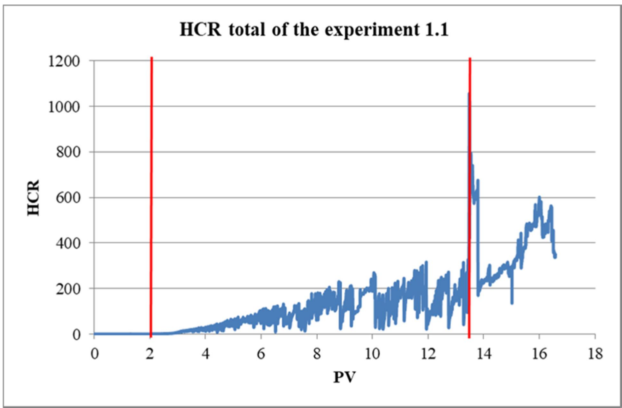

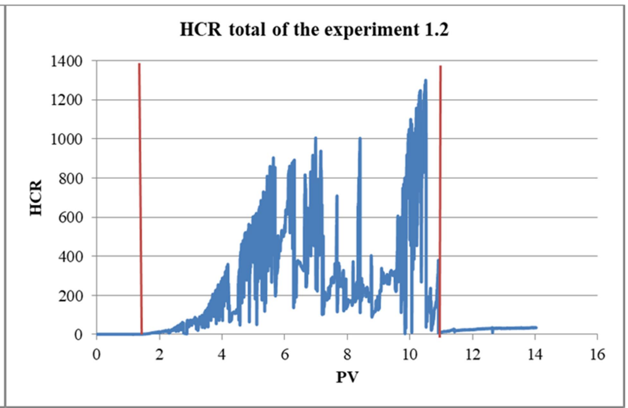

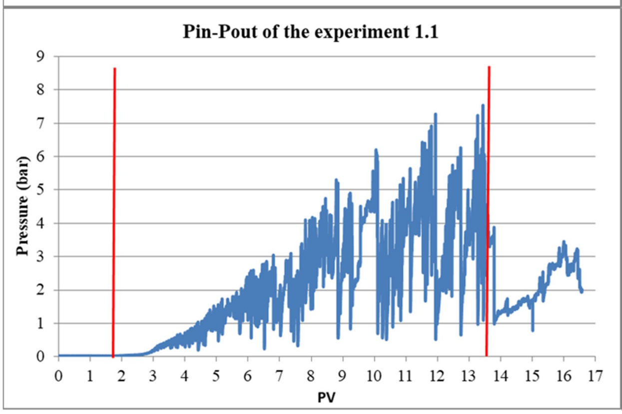

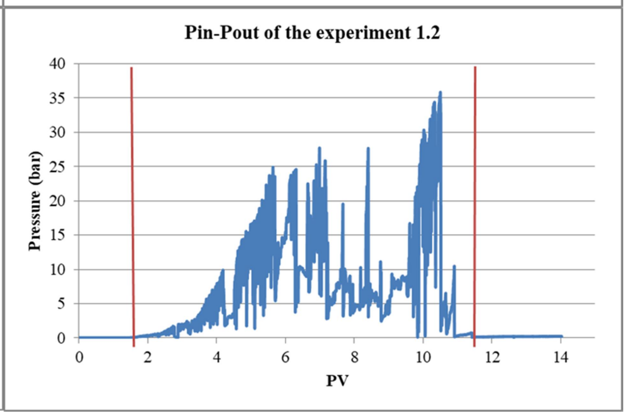

References

Benmebarek, N., Benmebarek, S., & Kastner, R. (2005). Numerical studies of seepagefailure of sand within a cofferdam. *Computer and Geotechnics*, pp. 264-273.

Bianco, C., Tosco, T., & Sethi, R. (2018). *MNMs 2018 Micro and Nanoparticles transport, filtration and clogging Model-Suite. A comprehensive tool for design and interpretation of colloidal particle transport in 1D Cartesian and 1D radial systems.*

Bonfiglio, C. (2017). *Hydraulic conductivity reduction induced by precipitation of aluminium-organic matter flocs in porous media.*

Bradford, S. A., Simunek, J., Bettahar, M., Van Genuchten, M. T., & Yates, S. (2003). Modeling Colloid Attachment, Straining, and Exclusion in Saturated Porous Media. *Environmental Science Technology*, pp. 2242-2250.

Bradford, S. A., Yates, S. R., Bettahar, M., & Simunek, J. (2002). Physical factors affecting the transport and fate of colloids in saturated porous media. *Water Resources Research*.

Costa, A. (2006). Permeability-porosity relationship: A reexamination of the Kozeny-Carman equation based on a fractal pore-space geometry assumption. *Geophysical research letters*.

Danka, J., & Zhang, L. M. (2015). Dike Failure Mechanisms and Breaching Parameters. *Journal of Geotechnical Geoenvironmental Engineering*.

de Moel, H., Bouwer, L. M., & Aerts, J. C. (2014). Uncertainty and sensitivity of flood risk calculations for a dike ring in the south of the Netherlands. *Science of the Total Environment*, pp. 224-234.

DeJong, J. T., Mortensen, B. M., Martinez, B. C., & Nelson, D. C. (2010). Bio-mediated soil improvement. *Ecological Engineering*, pp. 197-210.

Di Molfetta, A., & Sethi, R. (2012). *Ingegneria degli acquiferi.*

Duan, J., & Gregory, J. (2003). Coagulation by hydrolysing metal salts. *Advances in Colloid and Interface Science, 100-102*, pp. 475–502.

Elimeiech, M., & O'Meila, C. R. (1990). Kinetics of Deposition of Colloidal Particles in Porous Media. *Environmental Scence Technoogy 24*, pp. 1528-1536.

Fitts, C. R. (2013). *Groundwater Science.* Elsevier.

Gregory, J. (2006). *Particles in Water, Properties and Processes.*

Hagvall, K., Persson, P., & Karlsson, T. (2015). Speciation of aluminium in soils and stream waters: The importance of organic matter. *Chemical Geology, 417*, pp. 32–43.

Hopman, J. (2016). *First insights into Al-OM complexation and the effect of Al-OM flocs on porous media permeability.*

Hosseini, S. M., & Tosco, T. (2013). Transport and retention of high concentrated nano-Fe/Cu particles through highly flow-rated packed sand column. *Water Research 47*, pp. 326-338.

Jansen, B. (2003). *The mobility of aluminium, iron and organic matter in acidic sandy soils.*

Jarvis, P., Jefferson, B., & Parsons, S. A. (2005). Breakage, Regrowth, and Fractal Nature of Natural Organic Matter Flocs. *Environmental Science Technology, 39*, pp. 2307-2314.

Jarvis, P., Jefferson, B., & Parsons, S. A. (2006). Floc structural characteristics using conventional coagulation for a high doc, low alkalinity surface water source. *Water Research, 40*, pp. 2727 – 2737.

Jarvis, P., Jefferson, B., Gregory, J., & Parsons, S. A. (2005). A review of floc strength and breakage. *Water Research 39*, pp. 3121-3137.

Kleber, M., Eusterhues, K., Keiluweitk, M., Mikutta, C., Mikutta, R., & Nico, P. S. (2015). *Mineral-Organic Associations: Formation, Properties, and Relevance in Soil Environments.*

Laumann, S., Vesna, M., Lowry, G. V., & Hofmann, T. (2013). Carbonate minerals in porous media decrease mobility of polyacrylic acid modified zero-valent iron nanoparticles used for groundwater remediation. *Environmental Pollution*, pp. 53-60.

Lewis, J., & Sjöstrom, J. (2010). Optimizing the experimental design of soil columns in saturated and unsaturated transport experiments. *Journal of Contaminant Hydrology 115*, pp. 1-13.

Li, T., Zhu, Z., Wang, D., Yao, C., & Tang, H. (2006). Characterization of floc size, strength and structure under various coagulation mechanisms. *Powder Technology, 168*, pp. 104–110.

Logan, J. D. (2001). *Transport Modeling in Hydrogeochemical Systems.* Springer.

Luna, M., Gastone, F., Tosco, T., Sethi, R., Velimirovic, M., Gemoets, J., et al. (2015). Pressure-controlled injection of guar gum stabilized microscale zerovalent iron for groundwater remediation. *Journal of Contaminant Hydrology*, pp. 46-58.

Lundstrom, U. S., Van Breemen, N., & Bain, D. (2000). The podzolization process. A review. *Geoderma*, pp. 91–107.

McDowell-Boyer, L. M., Hunt, J. R., & Sitar, N. (1986). Particle Transport Through Porous Media. *Water Resourches Research*, pp. 1901-1921.

Mesticou, Z., Kacem, M., & Dubujet, P. (2016). Coupling Effects of Flow Velocity and Ionic Strength on the Clogging of a Saturated Porous Medium. *Transport Porous Media 112*, pp. 265-282.

Mulligan, C., Yong, R., & Gibbs, B. (2001). Remediation technologies for metal-contaminated soils and groundwater: an evaluation. *Engineering Geology*, pp. 193-207.

Nierop, K. G., Jansen, B., & Verstraten, J. M. (2002). Dissolved organic matter, aluminium and iron interactions: Precipitation induced by metal/carbon ratio, pH and competition. *The Science of the Total Environment 300*, pp. 201–211.

Pettit, E. R. (2014). Organic matter, humus, humate, humic acid, fulvic acid and humin: their importance in soil fertility and plant health. *Igarss*, pp. 1-17.

Pilarczyk, K. W. (1998). *Dikes and Revetments. Design, maintenance and safety assessment.* Taylor & Francis.

Ryan, J. N., & Elimelech, M. (1995). Colloid mobilization and transport in groundwater. *Colloids and Surfaces*, pp. 1-56.

Sauer, D., Sponagel, H., Sommer, M., Giani, L., Jahn, R., & Stahr, K. (2007). Review Article Podzol: Soil of the Year 2007 A review on its genesis, occurrence, and functions. *Journal of Plant Nutrition and Soil Science*, pp. 1-17.

Scheel, T., Haumaier, L., Ellerbrock, R. H., Rühlmann, J., & Kalbitz, K. (2008). Properties of organic matter precipitated from acidic forest soil solutions. *Organic Geochemistry 39*, pp. 1439–1453.

Sharma, M. M., & Yortsos, Y. C. (1987). Transport of Particulate Suspensions in Porous Media: Model Formulation. *American Institute of Chemical Engineers*, pp. 1636-1643.

Sharp, E. L., Jarvis, P., Parsons, S., & Jefferson, B. (2006). The Impact of Zeta Potential on the Physical Properties of Ferric-NOM Flocs. *Environmental Scence Technology, 40*, pp. 3934-3940.

Syngouna, V. I., & Chrysikopoulos, C. V. (2011). Transport of biocolloids in water saturated columns packed with sand: Effect of grain size and pore water velocity. *Journal of Contaminant Hydrology*, pp. 301-314.

Tien, C., & Ramarao, B. V. (2013). Can filter cake porosity be estimated based on the Kozeny–Carman equation? *Powder Technology*, pp. 233-240.

Tosco, T., & Sethi, R. (2010). Transport of Non-Newtonian Suspensions of Highly Concentrated Micro- And Nano scale Iron Particles in Porous Media: A Modeling Approach. *Environmental Science Technology, 44*, pp. 9062–9068.

Tosco, T., Bianco, C., & Sethi, R. (2018). MNMs - Micro- and Nanoparticles transport, filtration and clogging Model - Suite. A comprehensive tool for design and interpretation of colloidal particle transport in 1D Cartesian and 1D radial systems.

Tosco, T., Bosch, J., Meckenstock, R. U., & Sethi, R. (2012). Transport of Ferrihydrite Nanoparticles in Saturated Porous Media: Role of Ionic Strength and Flow Rate. *Environmental Science Technology 46*, p. 4008−4015.

Tosco, T., Papini, M. P., Viggi, C. C., & Sethi, R. (2014). Nanoscale zerovalent iron particles for groundwater remediation: a review. *Journal of Cleaner Production, 77*, pp. 10-21.

Tufenkji, N., & Elimelech, M. (2004). Correlation Equation for Predicting Single-Collector Efficiency in Physicochemical Filtration in Saturated Porous Media. *Environmental Science Technology*, pp. 529-536.

Tufenkji, N., Miller, G. F., Ryan, J. N., Harvey, R. W., & Elimelech, M. (2004). Transport of Cryptosporidium Oocysts in Porous Media: Role of Straining and Physicochemical Filtration. *Environmental Science Technology 38*, pp. 5932-5938.

Van Paassen, L. A. (2009). *Ground Improvement by Microbially Induced Carbonate Precipitation.*

Veerkamp, M. (2018). *The suitability of gibbsite as aluminum source to complex with dissolved organic matter.*

Wang, Y., Gao, B. Y., Xu, X. M., Xu, W. Y., & Xu, G. Y. (2009). Characterization of floc size, strength and structure in various aluminum coagulants treatment. . *Journal of Colloid and Interface Science, 332*, pp. 354–359.

Xu, Z. (2013). General report. Geotechnical problems of dikes (TC 201) and dams (TC 210) . *International Society for Soil Mechanics and Geotechnical Engineering*.

Yao, K. M., Hbibian, M. T., & O'Melia, C. R. (1971). Water and wastewater filtration. Concepts and applications. *Environmental Science & Technology*, pp. 1105-1112.

Yu, W. Z., Gregory, J., & Campos, L. (2010). Breakage and regrowth of Al-humic flocs - Effect of additional coagulant dosage. . *Environmental Science and Technology*, pp. 6371–6376.

Zhou, J., Laumann, S., & Heimovaaraa, T. J. (2019). Applying aluminum-organic matter precipitates to reduce soil permeability in-situ: A field and modeling study. *The Science of Total Environment 662*, pp. 99-109.

Zhou, J., Laumann, S., & Heimovaaraa, T. J. (in progress). Direct injection of aluminum-organic matter flocs to reduce soil permeability and create a vertical flow barrier in-situ.

Zhuang, J., Tyner, J. S., & Perfect, E. (2009). Colloid transport and remobilization in porous media during infiltration and drainage. *Journal of Hydrology*, pp. 112-119.